The Unfolded Protein Response and Cellular Toxicity: Implications in Neurodegeneration

BY

Zahra Mahmood

(NUST201361718MASAB92513F)

Atta-ur-Rahman School of Applied Biosciences,

National University of Sciences and Technology,

Islamabad, Pakistan.

The Unfolded Protein Response and Cellular Toxicity: Implications in Neurodegeneration

A thesis submitted as a final year project in partial fulfillment of the requirement for the degree of Masters of Science

By

Zahra Mahmood

(NUST201361718MASAB92513F)

Supervised by: Dr. Saadia Zahid

Atta-ur-Rahman School of Applied Biosciences,

National University of Sciences and Technology,

Islamabad, Pakistan.

2015

Dedicated to

My Beloved and much-missed

BABA

ACKNOWLEDGEMENTS

All praises to Almighty Allah, the authority of knowledge and creator of resources, skills and opportunities. Who guides me in congenital circumstances and blesses me to accomplish this work.

I am highly indebted to Dr. Saadia Zahid, my supervisor and a lifelong mentor. She has been highly patient with me. I thank her from the core of my heart that she did not give up on me and helped me fight and forge on ahead till I achieved all that I could. I am in gratitude to her wisdom and her guidance. I feel great honor to express my deep gratitude to Dr. Peter John, Principal, Atta ur Rahman School of Applied Biosciences (ASAB), for his efforts to keep the environment congenial for research and study. I am indebted to my external GEC member, Dr. Noreen Asim, University of Agriculture, Peshawar, for her invaluable suggestions. I also express my gratitude to my internal GEC members Dr. Aneela Javed and Dr. Touqeer Ahmed for putting up with the most inopportune queries. Moreover, I wish to express my genuine gratitude to Dr. Saima Zafar, University of Gottingen, for the facilitation of Tandem Mass Spectrometry and to Brig. Dr. Sohaib Hashmi and his team at the Armed Forces Institute of Pathology (AFIP), for providing us with the facilities for histological assessment of our samples.

My parents being next in line, I thank my beloved mom for all her support and consistent nagging (Thanks Maa). If my baba were here I hope he would be proud of me, as I am all that he taught me. (Miss you baba). I am thankful to my parents and their trust in me. This also goes for my siblings, Meerah Hafeez and Ahmed Mahmood, thanks for being there when I needed to vent out.

A bundle of thanks to my laboratory partner Sara Ahmed, whose company and support made me last this long. I owe you a big one.

A great many thanks to a special few who stood with me through my panic attacks, Nida Ali Syed, Sana Ayub, Aimen Saleem, Anum Hubab Hashmi and Naziha Khalid. I also

owe a big thank you to Muhammad Saalim, Muhammad Saeed, Abdul Haseeb Khan and Shahid Mahmood for their support in turbulent times.

My gratitude extends to my friend Nayyab Nawaz, who made me stick to my schedule and my deadlines.

Lastly, I would also wish to express my gratefulness to my Laboratory fellows and seniors, Maryam Masood, Ayesha Ali, Ammra Mahboob, Ghazala Iqbal, Mahpara Farhat and Habiba Butt for their consistent support and love.

Zahra Mahmood

Table of Contents

List of Figures

List of Tables

List of Acronyms

%	Percentage
ºC	Degree Celsius
Aβ	Amyloid beta
AD	Alzheimer's disease
ER	Endoplasmic Reticulum
APP	Amyloid precursor protein
CNS	Central nervous system
HCl	Hydrochloric acid
H_2O_2	Hydrogen peroxide
IRB	Internal review board
Kg	Kilogram
DTT	Dithiothreitol
IRE1	Inositol Requiring Endonuclease 1
BiP	Binding immunoglobulin Protein
PERK	PKR-like ER Kinase
ATF6	Activating Transcription Factor 6
TM	Tunicamycin
UPR	Unfolded Protein Response
ERAD	Endoplasmic Reticulum Associated Degradation
mg	Milligram
MS/MS	Tandem Mass spectrometry
PBS	Phosphate buffer saline
PCR	Polymerase chain reaction
RNA	Ribonucleic acid
ROS	Reactive oxygen species
rpm	Rotations per minute
ug	Microgram

Abstract

Endoplasmic reticulum (ER) dysfunction has an imperative role in numerous neurological disorders, including, multiple sclerosis, amyotrophic lateral sclerosis, prion diseases and Alzheimer's disease. In disease state, protein misfolding in the endoplasmic reticulum (ER) initiates a stress response, the unfolded protein response (UPR) in neurons due to a rise in proteotoxicity. Although there is an immense effort to explore the pathogenesis of ER dysfunction, unfortunately the exact mechanism is still unclear. Therefore as a preliminary initiative the present study was conducted to investigate one of the aspects of this complex molecular event. The study elucidates the molecular relationship between the unfolded protein response (UPR) during ER stress and aggregation of Amyloid beta that ultimately results in neuronal toxicity leading to neurodegeneration. The experimental animals, Balb/c mice were divided into 4 groups (n=15, each). Dithiothreitol (DTT) was used to induce UPR following ER stress. An optimum dose of DTT (75 mg/kg) was administered after every 24 hours. Histological examination showed a marked formation of amyloid beta plaques in the cortex and hippocampus sections of mice brain along with atrophied neuronal morphology, after 48 to 72 hours of treatment. Differential proteomic analysis was carried out using SDS-PAGE followed by ESI-QTOFMS/MS identification. The analysis revealed 10 differentially expressed cortical and hippocampal proteins, involved in various cellular and metabolic pathways. The gene expression analysis performed by Real-Time PCR determined the transcriptional expression of Activating Transcription Factor 6 (ATF6), a UPR regulating protein, and Amyloid Precursor Protein (APP) isoforms (common, 695 770). Furthermore, the immunohistochemical analysis also revealed the nuclear localization of ATF6 during ER stress. In conclusion, the findings of the present work may contributes to the existing pool of knowledge and provide a better understanding of complex molecular association of UPR with AB neurotoxicty that may help in further

elucidation of plausible aberrant molecular/signaling pathways during ER stress that may lead to neurodegeneration.

Chapter 1

Introduction

Neurodegeneration is a broad term encompassing the progressive loss of the structure and function of neurons. The disorders based on loss of neurons are termed as neurodegenerative disorders and include, Alzheimer's Disorder (AD), Parkinson's Disease (PD), Huntington's, among others. AD is the most common and is the 9th leading cause of mortality worldwide. One of the common hallmarks of neurodegenerative diseases is the aggregation of misfolded proteins. In AD, it is the formation of Amyloid beta (Aβ) plaques or Neurofibrillary Tangles (NFT's).

Stress like oxidative stress, heat shocks and environmental toxins have been implicated in initiating non-autonomous pathways against proteotoxicity. Proteotoxicity and proteostasis regulate one another inversely. Proteotoxicity causes a sharp decline in proteostasis and this decline causes misfolding of proteins and their aggregation. Proteotoxicity in turn leads to neurotoxicity and eventually neurodegeneration (Taylor et al., 2014).

The mammalian brain is highly vulnerable to oxidative damage, caused by excessive oxygen consumption, high iron content, low anti-oxidative enzyme activities or the abundance of polyunsaturated fatty acids in cell membranes (Youdim, 1988; Kowzlowski et al., 2012; Rouault, 2013).

In the presence of oxidative stress, free radicals surpass the capacity of the antioxidant defense and cause cellular dysfunction, degradation of the cell membrane and apoptosis (Campbell et al., 2001; Dixon and Stockwell, 2014). Protein oxidation evoked by these free radicals may cause protein structural and functional disruptions, and in this way are involved in age-related functional decline in the brain. Additionally, ROS are also

responsible for the formation of protein carbonyl formation by oxidizing amino acid residues, which cause cellular damage (Crichton et al., 2012). Oxidative stress has been established as a long-standing precursor of the formation of β-amyloid (Aβ) plaques in AD. There are two kinds of Aβ peptides; soluble and insoluble. The soluble β-amyloid protein is constantly being expressed in neurons and is cytoprotective in nature. Furthermore, it's over expression leads to its insoluble form, Aβ plaques or aggregates, which cause cell cycle arrest, degeneration and cell death (Butterfield, 1997; Butterfield and Boyd-Kimball, 2004; Castellani et al., 2012; Greenough et al., 2013). Moreover, it additionally connects with SOD1 and disrupts its enzymatic action.

The Unfolded Protein Response (UPR) is a last stage defense mechanism against prolonged cellular stress. It should be noted that the stress agent could be environmental or chemical (Wang and Kaufman, 2012). The UPR is enacted by the aggregation of unfolded/misfolded proteins in the endoplasmic reticulum (ER). The UPR is a homeostatic reaction to alleviate ER stress through transcriptional and translational events that diminish the generation of secreted and membrane proteins and enhances the production of chaperone molecules, foldases and the other various components included in ERQC and ERAD pathways. These are representations of cell-surviving mechanisms. Moreover, in the event that they come up short, then programed cell death (PCD) may result (Ron and Walter, 2007). While the UPR signaling pathways have been fundamentally worked out in yeast and mammals, similar pathways have been recognized in plants in recent years (Deng et al., 2013).

Mammalian systems have three types of UPR sensors, Inositol Requiring Endonuclease 1 (IRE1), PKR-like ER kinase (PERK) and Activating Transcription Factor 6 (ATF6). These three sensors are present on the ER membrane. Initiation of these three arms of the UPR relies on the Binding Immunoglobulin Protein (BiP). In their inactive state, the luminal areas of IRE1, PERK and ATF6 are connected with BiP (Bertolotti and Ron, 2001). When the cell encounters stress conditions, i.e. ER stress, BiP is contended far

from these anxiety sensors by an abundance of unfolded/misfolded proteins, bringing about the oligomerization of IRE1 and PERK and the translocation of ATF6 to the Golgi complex (Shen et al., 2002; Credle et al., 2005; Moore and Hollien, 2012).

ATF6 in mammalian cells is a type II ER membrane protein with two domains; a bZIP domain that faces the cytoplasmic side of the ER membrane and a Site-1-Protease (S1P) recognition domain, facing the ER lumen. Undergoing ER stress, ATF6 translocates from ER to the Golgi helped by the ER export machinery, coat protein complex II (COPII). ATF6 is subjected to sequential cleavages by a soluble luminal protease, S1P, and Site-2-Protease (S2P), which causes the cytoplasmic part of ATF6 to be released (Schindler and Schekman, 2009). This procedure is called regulated intramembrane proteolysis (RIP). The cleaved ATF6 travels into the nucleus and functions as a transcription factor (TF) activating the target genes expression. ATF6 initiates the UPR by directly interacting with the promoters of ERQC/ERAD related genes (Ye et al., 2000).

The UPR is typically instigated *in vitro* by treating the model with ER stress agents, like tunicamycin or DTT, where tunicamycin propels ER stress by hindering the exchange of oligosaccharides with nascent ER proteins (Hoyer-Hansen and Jaattela, 2007). Dithithreitol, $C_4H_{10}O_2S_2$ (DTT) is the commonly known as Cleland's reagentis a uniquely powerful reducing agent and when it undergoes oxidation, it conforms into a stable six-membered ring, with a core disulphide bond (S=S) (Cleland, 1964). DTT acts by disrupting the redox conditions required for the development of disulfide bridges in proteins.

DTT initiates ER stress by disrupting the redox conditions required for the formation of disulfide bridges in proteins (Ryoo et al., 2007). It ought to be called to attention that while both TM and DTT bring about misfolded protein conformations amassing in the ER, they are essential intermediaries for the characteristic natural conditions that evoke the UPR in cells. The current study proposes to observe the underlying mechanism of

key UPR players and toxic amyloid beta aggregation by inducing ER stress in a mouse model by using advance genomics and proteomics approaches.

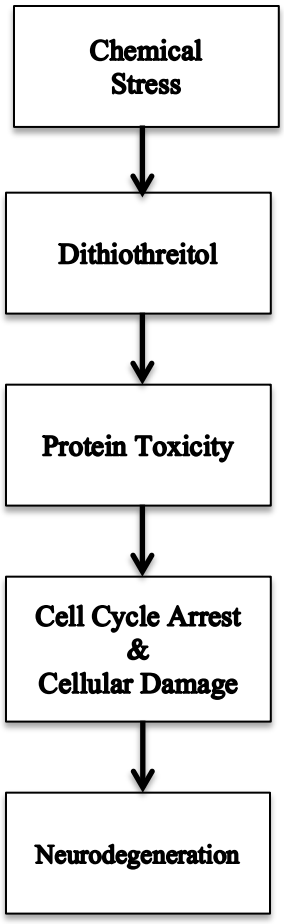

Figure 1.1: Mechanistic representation of chemically induced ER stress leading to Neurodegeneration. There are environmental and chemical sources causing cellular proteotoxicity in the mammalian brain, which in turn leads to neurodegeneration.

1.1 Research Objectives

The objectives of the study are;

- To observe the relationship between the unfolded protein response (UPR) and Aβ accumulation under ER stress conditions in mice cortex and hippocampal regions.
- To compare the ER stress levels with UPR regulating proteins in a time dependent manner by,

a. Cortical and hippocampal histopathological examination using Cresyl violet, congo red and Haematoxylin and Eosin (H&E) staining and immunohistochemical labeling of UPR regulator, ATF6 in the neurons.

b. Transcriptional analysis of genes mediating UPR and Aβ generation, that are, ATF6, APP common, APP 695 and APP 770 respectively.

c. Mapping differential cortical and hippocampal brain proteome under ER stress.

Chapter 2

Literature Review

2.1 The Unfolded Protein Response (UPR) in the Endoplasmic Reticulum (ER)

Neurodegenerative disorders like Alzheimer's Disease (AD), Parkinson's infection (PD), prion disease, Huntington's disease (HD), frontotemporal dementia (FTD), and amyotrophic lateral sclerosis (ALS) are portrayed by the accumulation and conglomeration of misfolded proteins. The aggregated proteins found in different regions of the brain are distinctive for each neurodegenerative disease. The foremost site of protein synthesis is the endoplasmic reticulum (ER), where secretory, transmembrane and organelle-targeted proteins are produced, comprising of nearly 30% of the proteome. A key component of protein quality control in the ER is the unfolded protein response (UPR), which is possibly the most important factor in play, if the proteostasis in the ER is aggravated (Scheper and Hoozemans, 2015).

Before the UPR was discovered, it had been observed that distinctive sorts of cellular stress like viral transformation; inhibition of glycosylation and calcium ionophore treatment induced the expression of a select group of proteins. These proteins were called glucose-regulated proteins (GRPs) in light of their induction by glucose deprivation and to distinguish them from a related group of proteins that were induced by temperature fluctuations, the heat shock proteins (Hsp) (Subjeck and Shyy, 1986). The term UPR was coined in 1988, when first direct association between protein folding stress in the ER and the induction of GRPs, including GRP78 (BiP), was made by overexpression of mutant influenza hemagglutinin protein in mammalian cells (Kozutsumi et al., 1988). This stress response was dubbed as the unfolded protein response or UPR. Gradually, the key signaling protein molecules that mediate the response were identified, with most of the pioneering work done in yeast (Mori et al., 1992). This was followed by the identification

of the sensors in the ER membrane responsible for transducing the signal from the misfolded proteins in the ER to the nucleus (Cox et al., 1993; Maly and Papa, 2014). These are three trans-membrane proteins present on the membrane of the ER, namely Inositol Requiring Enzyme 1 (IRE1), Protein kinase R (PKR)-like endoplasmic reticulum kinase (PERK) and Activating Transcription Factor 6 (ATF6). Under normal conditions, GRP78 or BiP binds these proteins at the ER membrane; however, under stress GRP78 releases the proteins, which in turn activate their own signaling mechanisms (Roussel et al., 2013).

2.2 The Unfolded Protein Response (UPR) Sensors

IRE1 oligomerizes when the response is activated which brings about trans-autophosphorylation. A primary consequence of activation of IRE1 is the unconventional splicing of XBP1 mRNA, bringing about the activation of the transcription factor XBP1 (Yoshida et al., 2001; Calfon et al., 2002; Lee et al., 2002). Mammalian cells, under stress, the protein synthesis is inhibited by the phosphorylation of the translation initiation factor eIF2α, which is catalyzed by protein kinase R (PKR)- like endoplasmic reticulum kinase (PERK), an ER transmembrane protein (Shi et al., 1998; Harding et al., 1999). Activating transcription factor 6 (ATF6) was the third sensor to be discovered. This membrane bound transcription factor is transported to the Golgi upon UPR activation where it is processed and released towards the nucleus (Haze et al., 1999). The IRE1, PERK and ATF6 pathways together comprise of an intricate network that has an expansive scope of transcriptional and translational targets. The UPR is closely associated with the proteolytic machinery of the cell. Proteins that misfold in the ER are sent out to the cytosol and degraded by the proteasome (Ruggiano et al., 2014). Then again, once the UPR is activated, autophagy increases and this turns into the major proteolytic system (Bernales et al., 2006; Ogata et al., 2006; Ding et al., 2007; Nijholt et al., 2011; Scheper et al., 2011). However, numerous mechanistic details and regulatory pathways are still uncovered, the core signaling factors involved in mammalian UPR had

been reported by 2002, as shown in figure 2.2. An important function of the UPR is its function as a proteostatic stress response initiated by ER dysfunction.

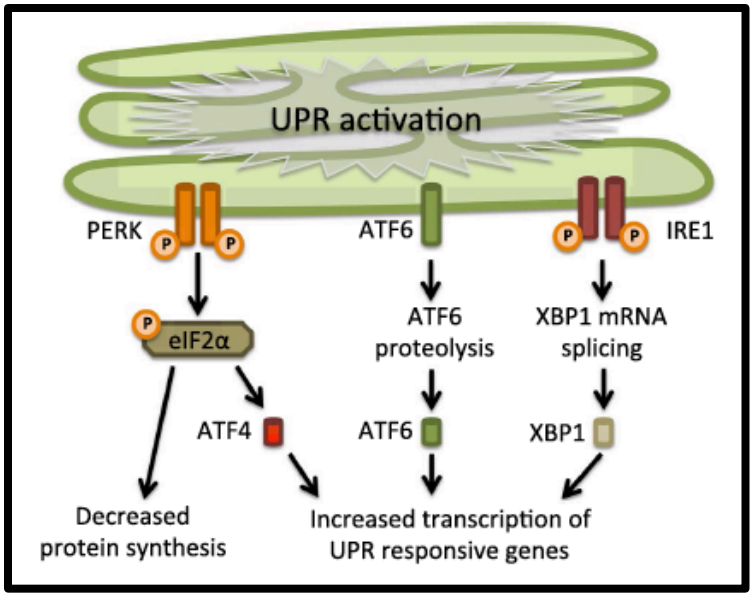

Figure #2.1: The unfolded protein response. The unfolded protein response consists of three independent signaling pathways that work in parallel and are activated upon accumulation of unfolded proteins inside the ER. Each signaling pathway is defined by the different ER-resident transmembrane proteins that act as ER stress sensors: RNA-activated protein kinase R (PKR)-like ER kinase (PERK), activating transcription factor 6 (ATF6) and inositol requiring enzyme 1 (IRE1). Activation of the UPR leads to an overall translational block and specific activation of ER stress responsive genes, which will increase the protein folding capacity and decrease the protein-folding load in the ER.

2.3 Dysfunction Of The Unfolded Protein Response (UPR)

Unsurprisingly, the dysfunction in the UPR can give rise to disease (Scheper and Hoozemans, 2015). In neurodegenerative disorders UPR initiation and activation is associated with ER dysfunction and prompts the loss of neuronal function. It is necessary to be aware of the diverse appearances that the UPR has in physiology and pathology.

The accumulation of misfolded proteins is a typical factor in neurodegenerative diseases (Roussel et al., 2013). Hence, it is noteworthy that the UPR has been extensively studied in respect to neurodegeneration, both in vivo and in vitro models. However, it is becoming apparent that the role of the UPR observed in these models is not consistent and even paradoxical. The proposed function of the UPR concluded from these models is difficult to connect to the human brain under pathological conditions (Hoozemans et al., 2005).

2.4 The Unfolded Protein Response (UPR) And Alzheimer's Pathology

Alzheimer's disease is an age-dependent neurodegenerative disease, one of the most common forms of dementia and the 9th leading cause of mortality. The neuropathological hallmark of AD is the accumulation of misfolded proteins; extracellular senile plaques of Aβ and intracellular aggregates of tau protein in the form of neurofibrillary tangles (NFTs). Hence, AD is the prime example of a protein folding disease (Taylor et al., 2002).

UPR specific markers are enhanced in AD brain tissue as compared to healthy brain tissue. GRP78 (BiP) levels are also increased in the hippocampus and cortical regions of the diseased brain. Moreover, other studies suggest the presence of phosphorylated PERK and IRE1 in AD neurons (Chang et al., 2002; Unterberger et al., 2006; Hoozemans et al., 2009; Stutzbach et al., 2013). These markers either appear in morphologically healthy neurons or in the neurons containing abnormally phosphorylated tau protein. However, haven't been observed in NFT containing neurons (Hoozemans et al. 2009). These observations indicate the involvement of the UPR in the early stages of AD.

2.5 Amyloid Precursor Protein (APP) and the Generation of Amyloid Beta Plaques (Aβ)

APP is a 695-770 amino acid membrane-spanning glycoprotein known to expressive in the brain and other various tissues (Nishimoto et al., 1993). APP assumes a major role in neuronal synapse formation and repair (Priller et al., 2006) and is likewise included in cell adhesion, cell signaling and long term potentiation. APP expression is high amid neuronal differentiation and after neural damage (Zheng and Koo, 2006).

APP processing results in Aβ creation that is the hallmark of neurodegeneration. The APP gene has 300,000 base pairs located on chromosome 21 (Preece et al., 2004). A total number of 18 exons can be alternatively spliced from the APP gene to produce distinctive isoforms (Hattori et al., 1997). The classification of APP isoforms is done on the premise of the absence or presence of exon 7, which encodes Kunitz type serine protease inhibitor (KPI) domain. APP751, APP770, APP365 and APP563 isoforms are KPI+ while APP695 and APP714 are KPI- isoforms (Preece et al., 2004). The numbers allude to the number of amino acids in each isoform. The APP isoforms having the KPI domain are over expressed and play an important role in AD pathology (Kitaguchi et al., 1988). APP770 and APP751 are plentifully expressed in astrocytes and microglia while APP695 is expressed in neurons (Leblanc et al., 1991). Changes in the expression pattern of APP isoforms in the brain mimics the changes in cellular density. Neuronal loss in AD brings about a decline in the APP695 isoform. Moreover, inflammation causes the activation of astrocytes thus causing an over expression of APP770 (Kitaguchi et al., 1990). APP is processed by the means of two proteolytic pathways; firstly α-secretase cleaves the middle of the Aβ sequence, producing a smaller C-terminal section (p3) and an extracellular, soluble sAPPα. Secondly, generation of Aβ and a dissolvable sAPPβ also occurs by the amyloidogenic route sequential cleavage by β and γ secretases (Wolfe et al., 1999). γ-secretase can cleave at amino acid 40 or 42, 1–40 structure is typical yet 1-42 is plenteous if there should arise an occurrence of AD. Aβ (1-42) prompts lipid peroxidation, DNA and protein oxidation both in vitro and in vivo (Drake et al., 2003).

Aβ is a small soluble aggregate, equipped with the capability of being embedded into the lipid membrane and to produce ROS. The disruption of cellular homeostasis is an unwanted consequence of lipid peroxidation, which brings about cell membrane damage, alterations in the activity of transport systems, ion channels, regulated cell functions and ultimately neurodegeneration (Varadarajan et al., 2000).

2.6 Amyloid beta (Aβ) Toxicity

Aβ (1-42) is damaging to the cells both in vivo and in vitro (Pike et al., 1993), it aggregates spontaneously to shape low atomic weight oligomers; then short, flexible protofibrils and long, rigid fibrils—all in dynamic equilibrium with one another (Lambert et al., 1998). Factors involved in the aggregation and accumulation of Aβ include: the presence of metal ions, such as, iron, aluminum and zinc (Mantyh et al., 1993), high peptide concentration, acidic pH (Burdick et al., 1992), oxidative stress (Dyrks et al., 1992) and the presence of very specific phospholipid metabolites (Klunk et al., 1997). Aβ prompts apoptosis by means of DNA damage (Su et al., 1994) and alterations in the products of the caspase cleavage (Kitamura et al., 1998; Engidawork et al., 2001). Cell death mechanisms are majorly overlapping, potentially relying upon the bioenergetics status of the cell as well as the intensity of the stimuli.

2.7 Chemical Induction Of The Unfolded Protein Response (UPR)

The UPR can be induced in all cell types by various chemicals. Tunicamycin and thapsigargin were introduced as UPR initiating agents with respect to their modes of action (Hu et al., 2006). Tunicamycin inhibits N-linked glycosylation of nascent proteins and causes the cell cycle to arrest causing the cell to be in stress (Chan and Egan, 2005). On the other hand, thapsigargin, disrupts the calcium homeostasis of the cell, built up by the ER, by inhibiting the enzyme, Sarco/Endoplasmic Reticulum Ca^{2+}-ATPase (SERCA) (Ding et al., 2006). Brefeldin A has also been implicated as an initiator of the UPR, as a calcium homoestatic inhibitor (Kitamura, 2011). Besides these chemicals, diothiothreitol

(DTT) has also been established as the causative agent of UPR. DTT is a laboratory reagent known as Cleland's Reagent. Usually, it is used to denature proteins in techniques like SDS-PAGE. However, recently it has been used to induce the UPR in various cell lines, *C. elegans* and zebrafish. Dithiothreitol is a reducing agent and reduces the disulphide bridges by causing thiol formation between cysteine residues, which causes protein build up in the endoplasmic reticulum, which leads to the initiation of UPR (Cleland, 1964). DTT has been utilized as an ER stress inducer in numerous cell lines; Mouse Embryonic Fibroblasts, multiple myeloma cell line, β cell line, MIN6, rat β cell lines and human pancreatic β cells and plasma cells (Miyazaki et al., 1990; Asfari et al., 1992; Hohmeier et al., 2000; Schindler and Schekman, 2009; Chen et al., 2011; Schuiki et al., 2012; Gao et al., 2014). Furthermore, recently DTT has also been used to induce stress in a transgenic zebrafish model (Li et al., 2015).

Chapter 3

Materials and Methods

3.1 Chemical Reagents

Reverse transcriptase (RT), Deoxynucleotide triphosphate (dNTPs) and Taq polymerase were acquired from Fermentas (Thermo Scientific, USA). Trizol was obtained from Invitrogen (USA). Dithiothreitol (DTT) and all the other chemicals were procured from Sigma-Aldrich, USA, unless indicated otherwise.

3.2 Animals

BALB/c mice were obtained from National Institute of Health (NIH) Islamabad, Pakistan and housed in the Laboratory Animal House of Atta-ur-Rehman School of Applied Biosciences (ASAB), National University of Sciences and Technology (NUST). After acclimatization time of two weeks, the mice were bred and kept in cages at a steady temperature (25±2 ºC) and regular light-dark cycles (12-12 h). The mice were provided with distilled water and a standard regimen comprising of 30% crude protein, 9% crude fat, 4% crude fiber and 10% moisture. 20 male mice (35-45 g and 10-12 weeks of age) were utilized in the experiments.

3.4 Ethics Statement

The mice were housed in the Laboratory Animal House of Atta-ur-Rehman School of Applied Biosciences (ASAB), National University of Science and Technology (NUST), under a controlled environment. All the experiments performed were in compliance with the rulings of the Institute of Laboratory Animal Research, Division on Earth and Life Sciences, National Institute of Health, USA (Guide for the Care and Use of Laboratory Animals: Eighth Edition, 2011). The protocol was approved from the Internal Review Board (IRB) of Atta-ur-Rahman School of Applied Biosciences, NUST.

3.5 Study Design

The experimental animals were divided into 5 groups (n=15, each) and were provided with unadulterated food and water regimen. DTT was administered intraperitoneally as a cellular stress-inducing agent at three different time intervals.

Serial No.	**Group**	**Treatment**	**Duration (Days)**
1	Control	Normal Feed and Water Placebo i.p. Administration	4
2	Dithiothreitol Treated- 24 h	Normal Feed and Water i.p. Injection of 75mg/kg dose of DTT	1
3	Dithiothreitol Treated- 48h	Normal Feed and Water i.p. Injection of 75mg/kg dose of DTT	2
4	Dithiothreitol Treated- 72h	Normal Feed and Water i.p. Injection of 75mg/kg dose of DTT	3

Table 3.1: Experimental design. Untreated Balb/c mice were used as the control. Other groups were $AlCl_3.6H_2O$, 24 h DTT treatment, 48 h DTT treatment and 72 h DTT treatment. (n=15)

3.6 Histological Examination of Brain Regional Tissues

3.6.1 Tissue Perfusion/Fixation for Histological Assessment

Heart perfusion was performed in accordance with the protocol of (Gage *et al*., 2012). The excised brain tissue was then placed in 4% paraformaldehyde for 24h at 4˚C before being processed further for paraffin processing and embedding. After 24 h, the brain tissue was dehydrated through a series of alcohols (isopropanol), 70% (1h), 95% (1h),

and 100% (1h) before paraffin infiltration. The brain tissues were then placed in xylene (4h) and paraffin embedding was performed by keeping the tissue in molten paraffin (4h at 60 °C and left to solidify (4 ^{o}C) in mould (block formation) prior to cutting.

3.6.2 Cresyl Violet Staining

Tissue sections (3 µ) mounted on slides were de-paraffinized in xylene for 10 m before being rehydrated by 70% isopropanol (10m), and washed with dd H_2O (5m). Cresyl violet stain was poured over the tissues sections and left for proper staining (4m). The sections were then washed with dd H_2O and 70 % acid alcohol (2m) and later dried for 2h before being mounted with cover slips. The slides were visualized by inverted microscope (Labomed, USA) at 10X and 40 X resolutions. The images were captured by Pixel Pro™ image analysis software (Labomed, USA).

3.6.3 Congo Red Staining

The Congo red stain (working solution: 49.5 mL Congo Red (Stock) and 0.5 mL 1% NaOH)) was poured on the de-paraffinized brain sections and left for 20 minutes. The sections were washed with dd H_2O and alkaline alcohol for 2 minutes. The sections were then counterstained by haemotoxylin for 30 seconds and further washed with 70% isopropanol for 6 minutes and then with dd H_2O. After air-drying (1 h) the slides were mounted by cover slips and later visualized by inverted microscope (Labomed, USA) at 40 X resolution. The images were captured by Pixel Pro™ image analysis software (Labomed, USA).

3.6.4 Haemotoxylin and Eosin Staining (H&E)

Standard haematoxylin-eosin staining was performed on 5 µ tissue sections. Tissue was de-paraffinized and incubated for 8 minutes in Mayer's haematoxylin solution and

washed in water for 10 minutes. Sections were dipped in 95% ethanol and counterstained with eosin for 30 seconds.

3.6.5 Immunohistochemical Staining

Sagital sections (5 μ) of brain tissues were mounted on Poly Lysine coated adhesive slides. Following de-paraffinization, heat mediated antigen retrieval was performed by incubating sections for 35 minutes in sodium citrate (pH: 6). The sections were subsequently washed and incubated in 35% H_2O_2. To minimize non-specific labeling the sections were incubated for 10 minutes in 5% bovine serum albumin in PBS and later incubated overnight at 4 °C in 0.1% bovine serum albumin in PBS containing: mouse monoclonal antibody for ATF6 (1:100; ab11909). The sections were then washed and placed in 1:100 dilution of HRP conjugated anti-mouse IgG (ab97051) for 1 h at room temperature. The peroxidase reaction product was visualized by incubation in a solution containing 0.025% of 3,3′ diaminobenzidine (DAB, ab50185) for 10 minutes. Following haematoxylin counter staining, cover slips were mounted and sections were visualized by inverted microscope (Labomed, USA) at 20 X resolutions. The images were captured by Pixel Pro™ image analysis software (Labomed, USA).

3.7 Brain Dissection and Isolation of Cortex and Hippocampus

Mice were anesthetized and sacrificed consecutively by neck dislocation and the cortex and hippocampus, were dissected out and immediately frozen in the liquid nitrogen. These samples were stored at -80 ºC until further processing.

3.8 Protein Expression Studies

3.8.1 Protein Extraction

The entire tissue lysates were prepared by suspension in 100 µl of ice-cold lysis buffer (7M urea, 2M thiourea, 4% CHAPS, 10 mM Phenyl methyl sulfonyl fluoride (PMSF), 1% Dithiothreitol (DTT)), superseded by sonication utilizing an UP400S Ultrasonic Processor (Hielscher Ultrasound Technology). To increase dissolubility, the homogenates were placed at room temperature for 1 hour and centrifuged at 14000 rpm at 4 ºC for 10 min. The supernatant was collected and stored at -20 ºC. In order to maximize the yield, 50 µl lysis buffer was added to the pellet and the treatment was recapitulated. The two suspensions were pooled and centrifuged at 14000 rpm for 90 minutes. The last supernatant was stored at – 80 ºC until further use.

3.8.2 Protein Quantification (Bradford's Assay)

Serial dilutions of Bovine Serum Albumin (BSA) (1mg/1ml) were prepared with ddH2O. The samples were diluted with ddH2O (1:20) in duplicate. The total volume of every standard/example was 20 µl and 1 ml of Bradford's reagent was included, followed by a spin in the vortex. The samples were incubated for 10 min at room temperature. The absorbance of every sample was measured at 595 nm using OPTIMA 300 spectrophotometer. A standard curve was inferred by plotting standard absorbance against its concentration. This curve was used to quantify the protein concentration against the observed absorbance.

3.8.3 Protein Separation- Sodium Dodecyl Sulphate-PolyAcrylamide Gel Electrophoresis (SDS-PAGE)

Sodium Dodecyl Sulphate Polyacrylamide Gel Electrophoresis (SDS-PAGE) was utilized to separate the proteins based on their molecular weight. 10% resolving gel (distilled

water; monomer solution; 1.5M Tris-HCl pH 8.8; 10% SDS; 10% ammonium per sulphate; TEMED) was prepared and poured quickly between the glass plates. Isopropanol was added to the top and the gel was left to polymerize for 40 minutes. This was followed by the preparation of 4% stacking gel (distilled water; monomer solution; 1.5 M Tris-HCl pH 6.8; 10%SDS; 10%APS; TEMED). Stacking gel was poured on top of the polymerized resolving gel. The comb was immediately inserted into the gel. The gel was left for another 25 minutes to allow polymerization. After polymerization, the combs were removed and the glass plates were moved to the electrophoresis tank, which was loaded with 1X electrode tank buffer. Samples were prepared by the addition of sample diluting buffer (0.125M Tris-HCl pH 6.8; 20% Glycerol; 10% 2-Mercaptoethanol). The samples were heated at 100ºC for 2 min and given a short spin at 14000 rpm for 2 min. The samples were then loaded into the wells and the electrophoretic separation procedure was carried out at 100 millivolts for 90 min. After the run, the gel was put in coomassie brilliant blue staining solution (0.025%), overnight. The gel was destained, utilizing 10% destaining solution (75ml glacial acetic acid; distilled water; 25 ml of 100% ethanol) until a clear background was achieved.

3.9 Mass Spectrometry

Using a 22 min linear gradient (5-35% acetronitrile vs. 0.1% formic acid, 240 ml/min), the peptide mixtures were concentrated on a Reversed Phase-C18 pre-column (0.15 mm ID x 20 mm self-packed with Reprosil-Pur 120 C18-AQ 3 μm material) and then separated by Reversed Phase-C18 nano-flow chromatography (0.075 mm ID x 200 mm Picofrit column, packed with Reprosil-Pur 120 C18-AQ 3 μm material) on an EASY nLC-1000 system. The eluents were analyzed using a Top10 method in Data Dependent Acquisition mode on a Q Exactive high resolution mass spectrometry system operated under Tune 2.2 using HCD fragmentation, with a Normalized Collision Energy of 25%. Peak lists were generated using Raw2 MSM v1.10 software (MPI for Biochemistry, Martinsried).

3.10 Gene Expression Analysis

3.10.1 RNA Extraction

RNA extraction was done by the manufacturer's protocol utilizing Tri-reagent. Upon dissection, the brain tissue was immediately washed with phosphate buffer saline solution (1X PBS) and then homogenized in 1 ml trizol, utilizing a sonicator (UP400S Hielscher Ultrasound Technology). The homogenized tissue was placed at room temperature for 10 min to ensure nucleoprotein complex disassociation. 0.2 mL of chloroform was added and the sample tubes were shaken vigorously until the mixture turned milky and then were allowed to stand at room temperature for 10 min. The samples were then centrifuged at 12,000 rpm for 15 min at 4 ˚C. After centrifugation the upper aqueous phase was collected and transferred to another tube. 0.5 mL of isopropanol was added to the samples and then was allowed to stay at room temperature for 10 min. The samples were centrifuged again at 12,000 rpm for 10 min at 4 ˚C. The RNA precipitated and formed a pellet on the internal side of the tube. The supernatant was discarded and the pellets were washed with 1 ml of 75% ethanol. Furthermore, it was centrifuged at 7500 rcf for 5 min at 4 ˚C. The final RNA sample was stored at -80 ˚C until further processing.

3.10.2 Production of cDNA

For complementary DNA (cDNA) synthesis, the extracted RNA was centrifuged at 12000 rpm for 5 min. Pellet was permitted to dry and resuspended in 30µl of PCR water. RNA of all the samples (cortex and hippocampus) was run on 2% agarose gel to determine the quantity of RNA. RNA bands were visualized on Wealtech Dolphen Doc (S/N470883) Gel Documentation System. The RNA quality, as judged according to the ratio of 28S to 18S rRNA on the agarose gel was comparable among all samples.

Extracted RNA was quantified utilizing BioPhotometer Plus (Eppendorf, Germany) and equal quantities of RNA were utilized to reverse transcribe into cDNA. The protocol used for qRT-PCR reaction included, 3 µl of 10mM dNTP's, 3 µl of 5mM oligo dT, 8 µl of 5x RT buffer, 4 µl of 0.1M Dithiothreitol (DTT) and 2µl of MMLV-RT enzyme. Complete volume of the reaction mixture was made up to 40 µl by the addition of PCR water accordingly.

3.10.3 Reverse Transcriptase Polymerase Chain Reaction (RT-PCR) for cDNA Synthesis

RNA extracted was quantified using BioPhotometer plus (Eppendorf, Germany) and equal quantity of RNA was used to reverse transcribe in to cDNA. The protocol used for RT-PCR reaction included 4.5 µl of 10mM dNTP's, 4.5 µl of 5mM oligodT (heated for 5 min at 55 °C) 12 µl of 5x RT buffer, 6µl of 0.1M Dithiothreitol (DTT) and 3µl of MMLV-RT enzyme. Total volume of reaction mixture was made up to 60 µl by the addition of PCR water accordingly.

3.10.4 Gene Expression Analysis by Quantitative Real Time Polymerase Chain Reaction (qPCR)

Real time PCR was performed in ABI Prism 7300 Sequence Detection System (Applied Biosystem, 7300) by using SYBR Green PCR Master Mix. The PCR reaction mixture consisted of 12.5µl of SYBR Green PCR Master Mix, 1µl of both forward and reverse primer specific for particular genes, 3 µl of cDNA template and then volume was made up to 25µl by adding DNase water. The thermocycling conditions were 50 °C for 2 min, 95 °C for 10 min followed by 40 cycles of 30 sec at 95 °C, 1 min at 60 °C followed by 1 min at 72 °C, and a final dissociation step. Dissociation curves and agarose gel electrophoresis were used to verify the quality of the PCR products. All values were normalized to β-actin. Values obtained from three independent experiments were

analyzed relative to gene expression data using the $2^{-\Delta\Delta CT}$ method (Livak and Schmittgen, 2001). The specific primer sequences of β-actin, ATF6, APP common, APP 695 and APP 770 are listed in Table 3.2.

Serial No.	**Gene**	**Forward Primer Sequence (5'-3')**	**Reverse Primer Sequence (5'-3')**	**Amplicon (bp)**
1	ATF6	TGCCTTGGGAGTCAGACCTAT	GCTGAGTTGAAGAACACGAGTC	141
2	APP Common	TGTGATCTACGAGCGCATGAACC	AAGACATCGTCGGAGTAGTTCTGC	126
3	APP 695	GATGAGGATGTGGAGGATGG	GCTGCTGTCGTGGGAACTC	149
4	APP 770	TGCTCTGAACAAGCCGAGACC	CATGCAGTACTCTTCCGTGTC	144
5	Beta-Actin	GCCTTCCTTCTTGGGTATGG	CAGCTCAGTAACAGTCCGC	359

Table 3.2: Primer Sequences used for Expression Analysis of ATF6, APP common, APP 695 and APP 770

3.11 Image and Statistical Analysis

Image Lab™ software (Bio-RAD) was employed for gel image analysis, quantification and molecular weight calculation of the protein bands. The differential expression of proteins was calculated on the basis of relative quantity of each protein band. The data was statistically analyzed by One Way ANOVA. A value of $p < 0.05$ was considered to be statistically significant. The histograms for differential protein expression were generated with Graph Pad Prism 6.

3.12 In Silico Analysis of Functional Association

To investigate functional association network of identified differentially expressed proteins, their respective UniProtKB accession numbers was submitted in STRING 8.3 database (http://string-db.org/).

Chapter 4

Results

4.1 Comparative Histological Assessment of Neurodegeneration induced by DTT

The morphological changes occurred in the cortex and hippocampus after the administration of DTT, was assessed by Cresyl violet and congo red staining (Figure 4.1-4.2). The cresyl violet stain showed a marked decline of Nissl bodies in DTT treated groups. Similarly, the congo red stain expressed the presence of Amyloid beta aggregates. The results showed that Dithiothreitol, a potent ER stress inducer has caused neurodegeneration in the cortical and hippocampal regions. It was observed that at a dose of 50 mg/kg, the neuronal cells underwent slight morphological changes while there was a drastic loss of cellular morphology with prominent neurodegeneration at a dose of 100 mg/kg. However, at 75 mg/kg, the extent of neurodegeneration was moderate with significant alteration in cellular architecture. Therefore, a dose of 75 mg/kg was used as an optimum dose to induce ER stress. Furthermore, marked cellular degeneration was also seen after 72 hours of DTT administration, at a dose of 75 mg/kg in Haemotoxylin and Eosin (H&E) stained sections (Figure 4.3).

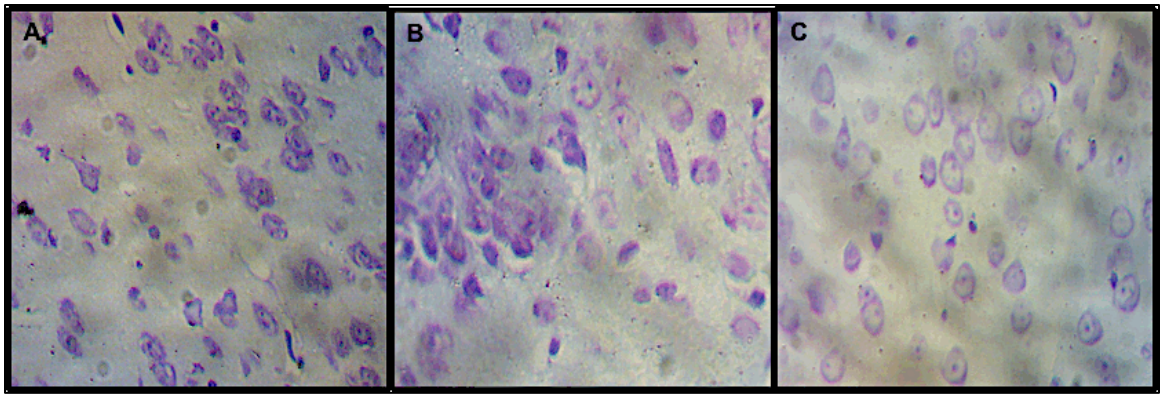

Figure 4.1: Histological assessment of DTT treated Mouse Brain sections by Cresyl Violet. Evaluation of the optimum dose from the different doses of DTT (Magnification: 40X). **A:** 50 mg/kg, **B:** 75 mg/kg, **C:** 100 mg/kg.

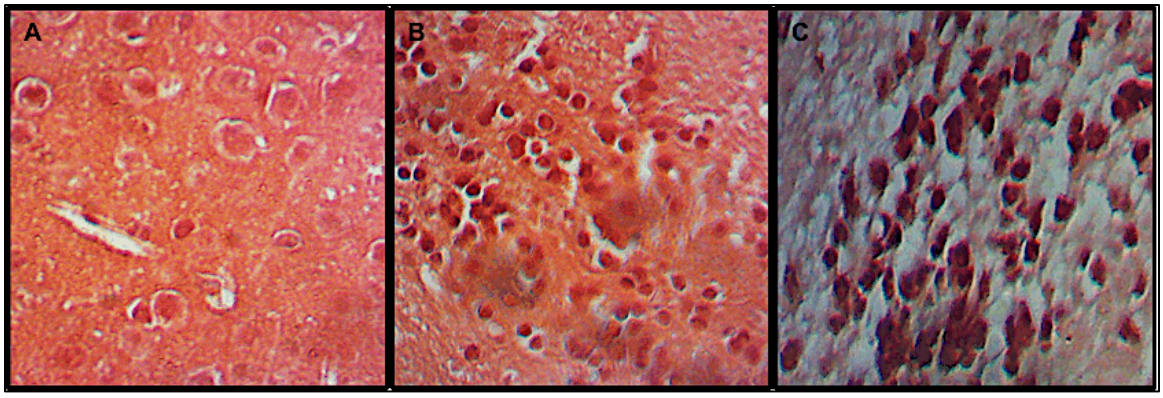

Figure 4.2: Histological assessment of DTT treated Mouse Brain sections by Congo Red. Evaluation of the optimum dose from the different doses of DTT (Magnification: 40X). **A:** 50 mg/kg, **B:** 75 mg/kg, **C:** 100 mg/kg.

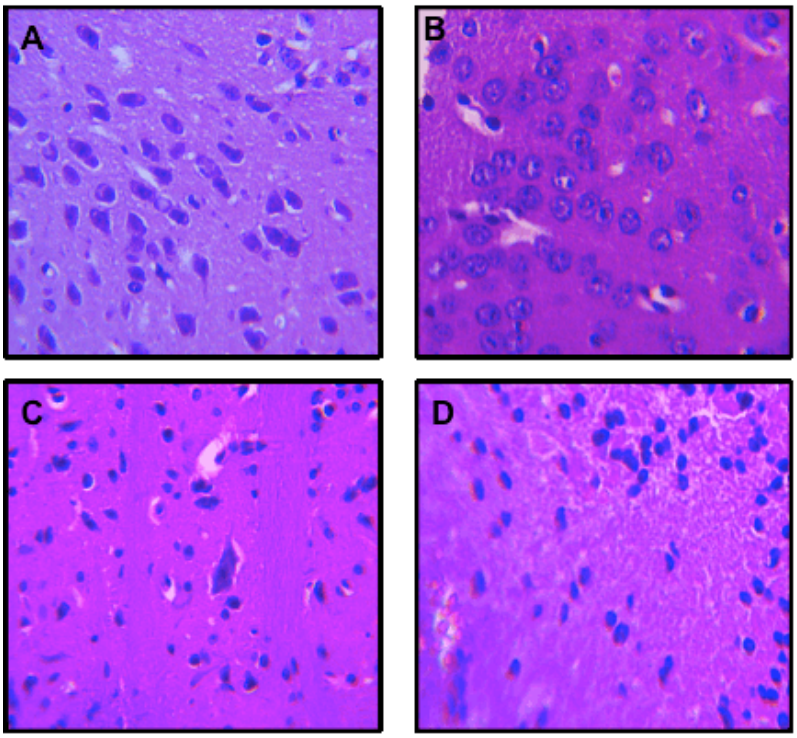

Figure 4.3: H&E staining of Mouse Cortex and Hippocampus. A: Control, **B:** 24 hours DTT-treated group, **C:** 48 hours DTT-treated group, **D:** 72 hours DTT-treated groups (Magnification: 40X).

4.1.1 Localization of activated ATF6

In normal physiological conditions, inactive ATF6 is found in the cytoplasm bound to BiP on the ER membrane. The results of immunohistochemistry show the translocation of ATF6 from the cytoplasm to the nucleus, after its activation under ER stress conditions. Specifically after 48 h of treatment, when ER stress was at its peak (Figure 4.4).

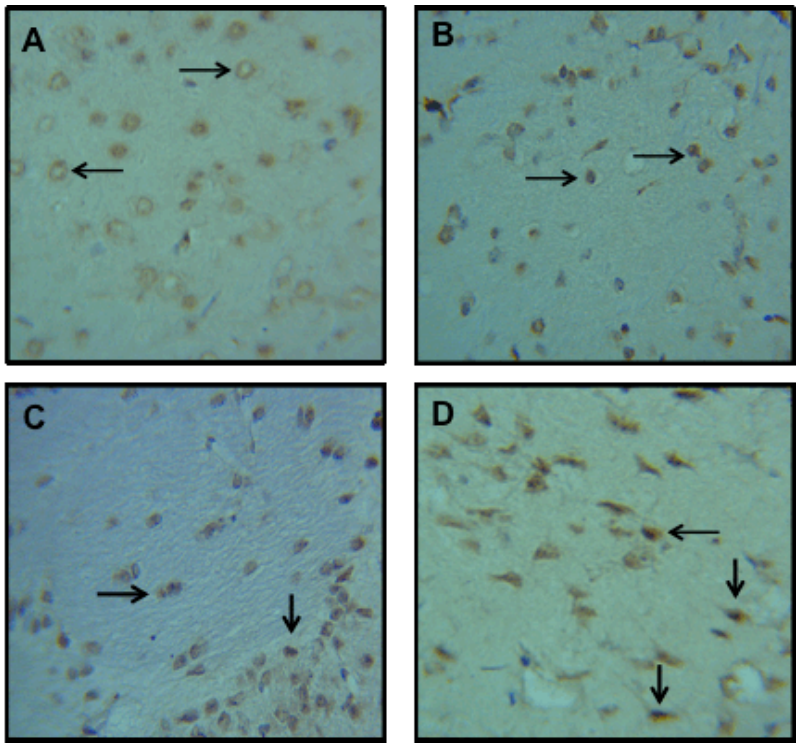

Figure 4.4: Immunohistochemical Observation of ATF6 Localization. The brain sections were fixed and stained with anti-ATF6 antibody and DAB, respectively. ATF6 immunoreactivity in the brain sections of Balb/c mice in different groups. (Magnification: 40X). **A:** Control, **B:** 24 hours DTT-treated group, **C:** hours DTT-treated group, **D:** hours DTT-treated group

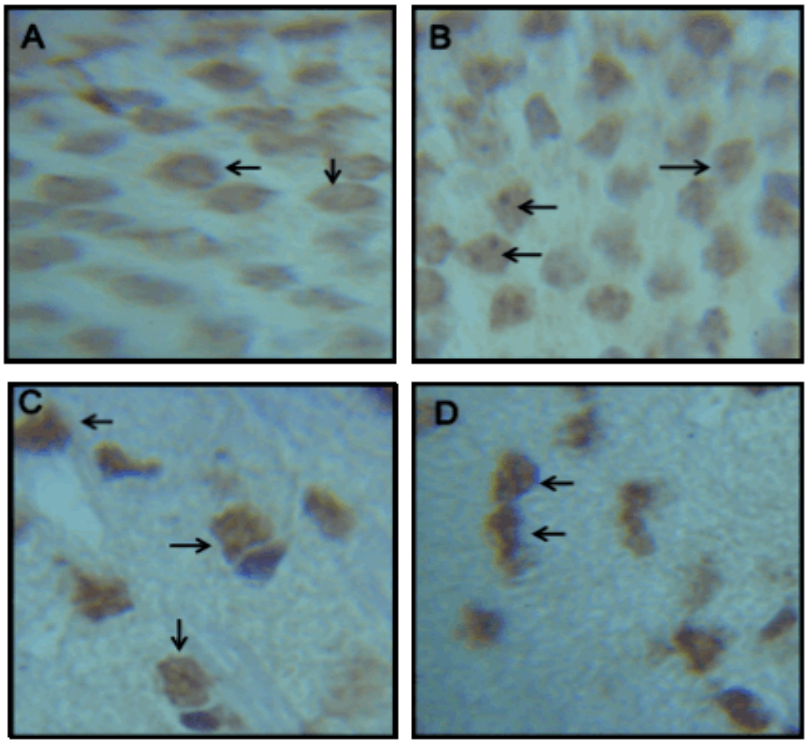

Figure 4.5: Immunohistochemical Observation of ATF6 Localization. The brain sections were fixed and stained with anti-ATF6 antibody and DAB, respectively. ATF6 immunoreactivity in the brain sections of Balb/c mice in different groups. (Magnification: 100X). **A:** Control, **B:** 24 hours DTT-treated group, **C:** hours DTT-treated group, **D:** hours DTT-treated group

4.2 Protein Quantification

Protein concentration of each sample was estimated by plotting the absorbance value of the colored reaction product on the standard curve. The intensity of the colored product is directly proportional to the protein content of the sample (Figure 4.5).

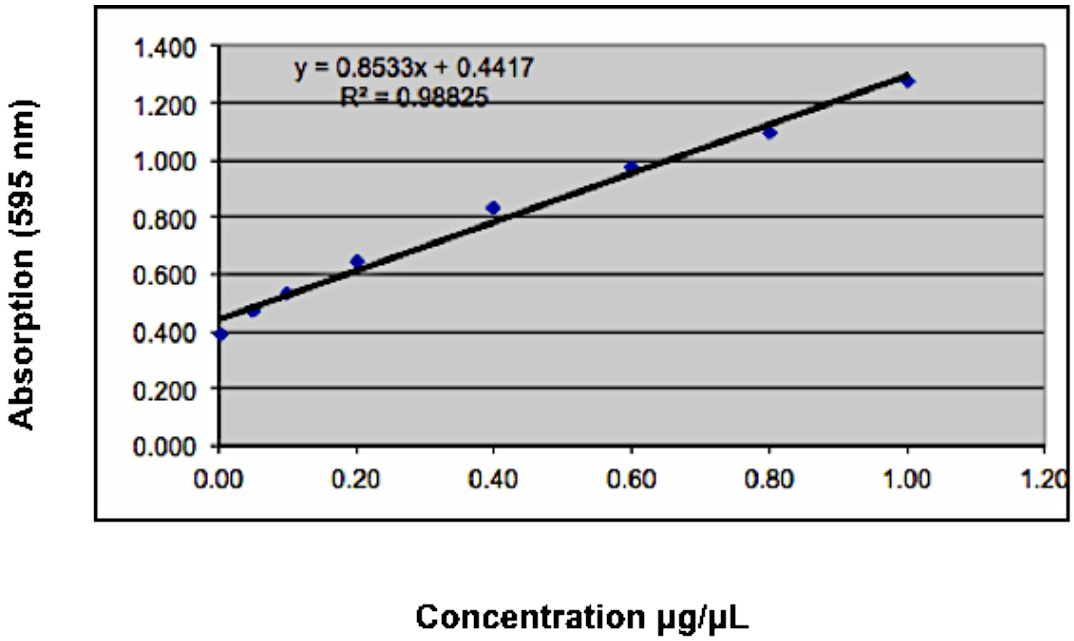

Figure 4.6: Bradford standard curve plotted for eight standard values. Concentration was plotted on the x-axis. Absorbance measured at 595 nm was plotted on the y-axis. This graph represents linear regression for eight standard points. The obtained linear regression value was 0.98825 (R2=0.98825).

4.2.1 Differential Expression Of Hippocampal And Cortical Proteins

The total proteome profile of the cortex and hippocampus for all four groups was obtained by 1D gel separation (SDS-PAGE). The gel image analysis was performed using Image Lab^{TM} software, which revealed a total of 10 differentially expressed protein bands (ANOVA, p-value<0.05) in the cortex and hippocampus (Figure 4.6A and 4.6B) (Table 4.1). Out of these 10 proteins, 2 cortical and 3 hippocampal proteins had exhibited significantly increased expression after 24 h of DTT treatment. Additionally, the expression of these proteins significantly declined after 48 h and 72 h of treatment respectively. These included NADH-Ubiquinone Oxidoreductase (cortex, figure 4.7), ATP Synthase subunit α (cortex and hippocampus, figure 4.8A and 4.8B), Glycerol-3-Phosphate Dehydrogenase, Fructose Bisphosphate Aldolase A and V-type Proton ATPase

subunit C (hippocampus, Figure 4.9-4.11). Ubiquitin-60S Ribosomal Protein L40 and Serum Albumin depicted a pattern of continuous decline in their expression in the cortex and hippocampus respectively (Figure 4.12-4.13). The expression of Neuromodulin and Succinate Semi Aldehyde Dehydrogenase were observed to significantly up regulate with the increase in the DTT dose in the cortex and hippocampus respectively. Calmodulin/calcium dependent kinase type II subunit α displayed an interesting pattern of expression in cortex, with significantly decreased expression in the first 24 h of treatment, however it an increase in expression was observed after 48 h, approximately to the expression levels found in the control group. But with the time span (72 h of DTT treatment) the expression level significantly declined to almost negligible level (Figure 4.16). Functional association network generated through STRING 8.3 also revealed a strong interaction among the identified differentially expressed proteins (Figure 4.17).

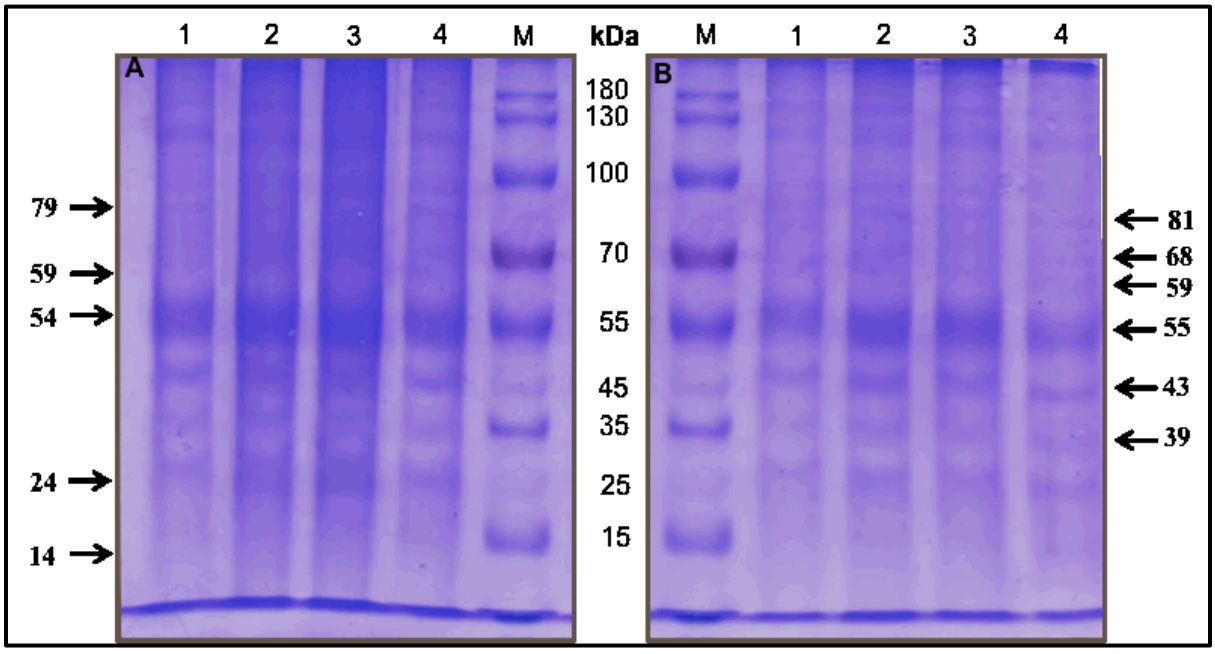

Figure 4.7: Proteome Mapping of Cortical and Hippocampal proteins. The extracted proteins were separated on 12% resolving gel and stained with Coomassie Brilliant Blue. The gel was visualized on ChemiDoc™. And analyzed by LabImage Software.

A: Cortex: Lane 1= Protein Marker (Thermo Scientific Page Ruler™), Lane 2= Control group, Lane 3= 24 hours DTT treated group, Lane 4= 48 hours DTT treated group, Lane 5= 72 hours DTT treated group. The amount of cortical protein extract, loaded in each well was 50µg.

B: Hippocampus: Lane 1= Protein Marker (Thermo Scientific Page Ruler™), Lane 2= Control group, Lane 3= 24 hours DTT treated group, Lane 4= 48 hours DTT treated group, Lane 5= 72 hours DTT treated group. The amount of cortical protein extract, loaded in each well was 50µg.

Accession Number	Protein	Mol. Wt. (kDa)	Peptide Matches	Percent Coverage (%)	Functional Category
Q91VD9	NADH Ubiquinone Oxidoreductase	79	18	29.70	Catalysis
Q03265	ATP Synthase, subunit α	59.7	33	70.70	Catalysis
Q64521	Glycerol-3-Phosphate Dehydrogenase	80.8	27	36.90	Metabolism
P05064	Fructose Bisphosphate Aldolase A	39.3	24	53.60	Metabolism
Q9Z1G3	V-type Proton ATPase, Subunit C	43	11	25.70	Catalysis
P62984	Ubiquitin-60S Ribosomal Protein L40	14.7	4	24.20	Protein Degradation
P06837	Neuromodulin	23.6	3	15.40	Nerve Growth
P07724	Serum Albumin	68	24	46.20	Cellular Transport
Q8BWF0	Succinate Semi Aldehyde Dehydrogenase	55.2	15	34.60	Catalysis
P11798	Calcium/ Calmodulin dependent kinase type II subunit α.	54.1	15	38.10	Catalysis

Table 4.1: Differentially expressed proteins during ER stress treated with DTT in mice cortex and hippocampus as identified by ESI-QTOF MS/MS. Accession number and functional categories have been obtained by UniProt and the percent coverage refers to the percentage of protein sequence coverage, determined by the number of matched peptides.

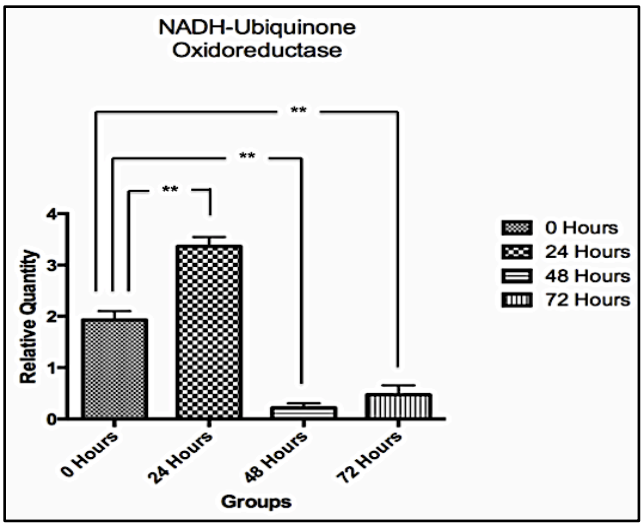

Figure 4.8: Differential Protein Expression of NADH-Ubiquinone Oxidoreductase. Expression detected in Control, 24 hours DTT-treated group, 48 hours DTT-treated group and 72 hours DTT-treated group. **p<0.01.

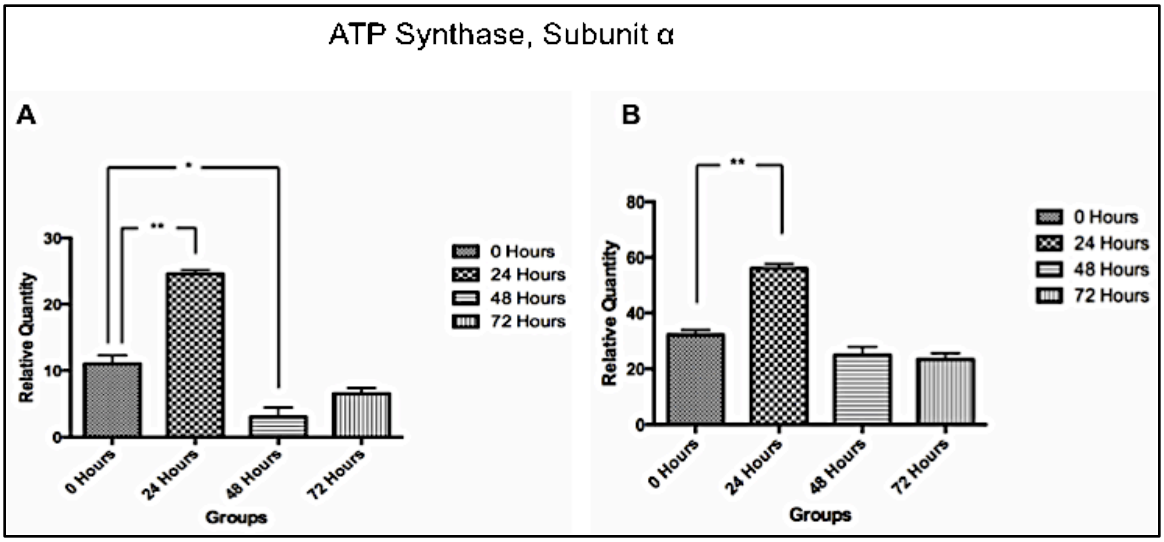

Figure 4.9: Differential Protein Expression of ATP Synthase, subunit α. A: Cortex and **B:** Hippocampus. Expression detected in Control, 24 hours DTT-treated group, 48 hours DTT-treated group and 72 hours DTT-treated group. *p<0.05, **p<0.01.

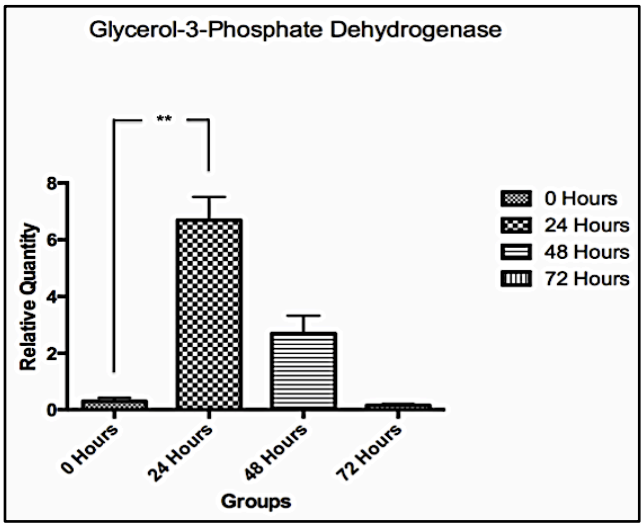

Figure 4.10: Differential Protein Expression of Glycerol-3-Phosphate Dehydrogenase. Expression detected in Control, 24 hours DTT-treated group, 48 hours DTT-treated group and 72 hours DTT-treated group. ***p*<0.01.

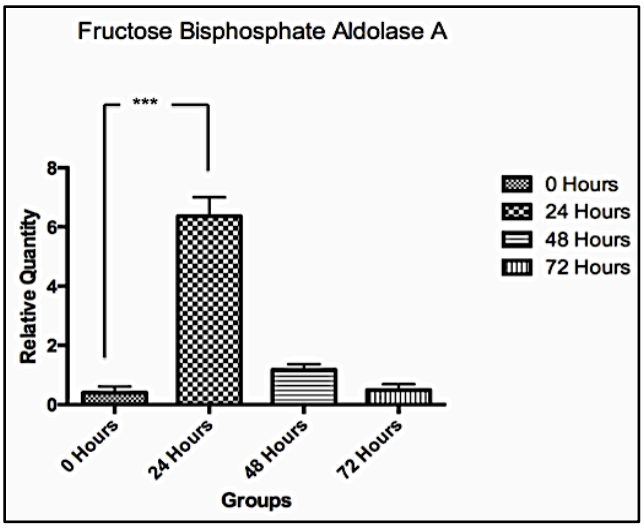

Figure 4.11: Differential Protein Expression of Fructose Bisphosphate Aldolase A. Expression detected in Control, 24 hours DTT-treated group, 48 hours DTT-treated group and 72 hours DTT-treated group. ****p*<0.001.

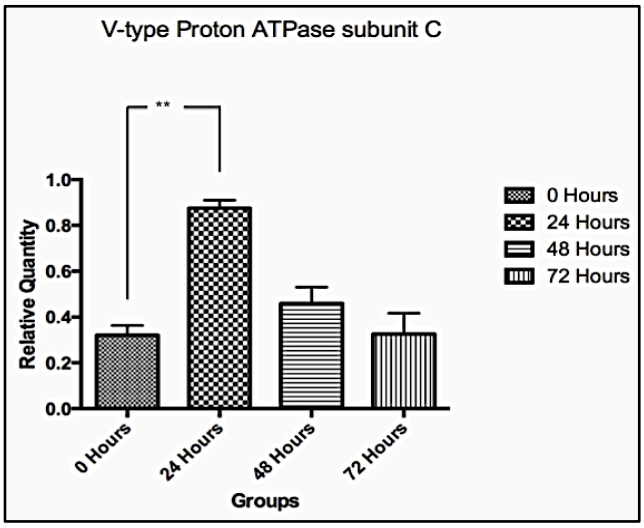

Figure 4.12: Differential Protein Expression of V-type Proton ATPase, subunit C. Expression detected in Control, 24 hours DTT-treated group, 48 hours DTT-treated group and 72 hours DTT-treated group. ***p*<0.01.

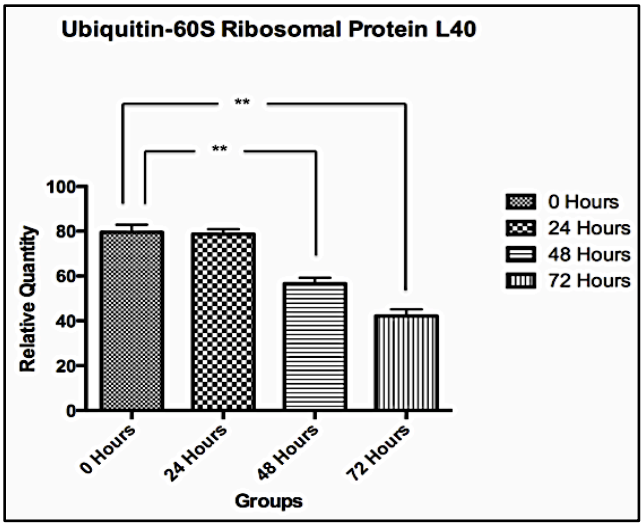

Figure 4.13: Differential Protein Expression of Ubiquitin-60S Ribosomal Protein. Expression detected in Control, 24 hours DTT-treated group, 48 hours DTT-treated group and 72 hours DTT-treated group. ***p*<0.01.

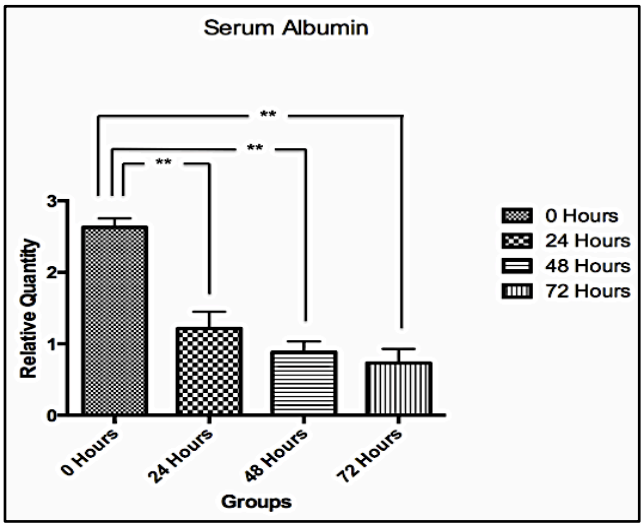

Figure 4.14: Differential Protein Expression of Serum Albumin. Expression detected in Control, 24 hours DTT-treated group, 48 hours DTT-treated group and 72 hours DTT-treated group. ** $p<0.01$.

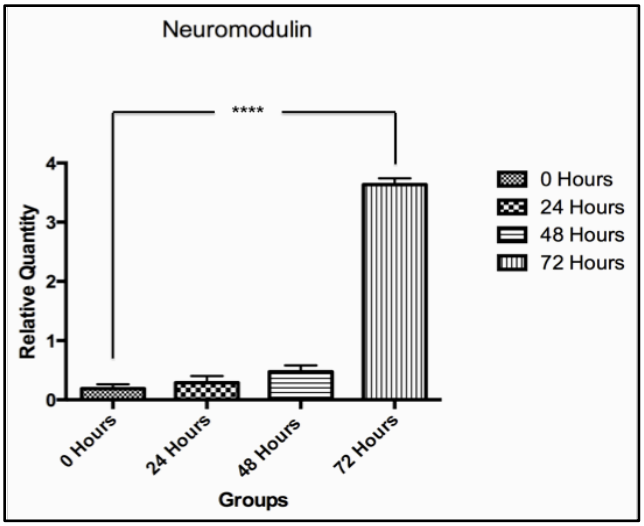

Figure 4.15: Differential Protein Expression of Neuromodulin. Expression detected in Control, 24 hours DTT-treated group, 48 hours DTT-treated group and 72 hours DTT-treated group. **** $p<0.0001$.

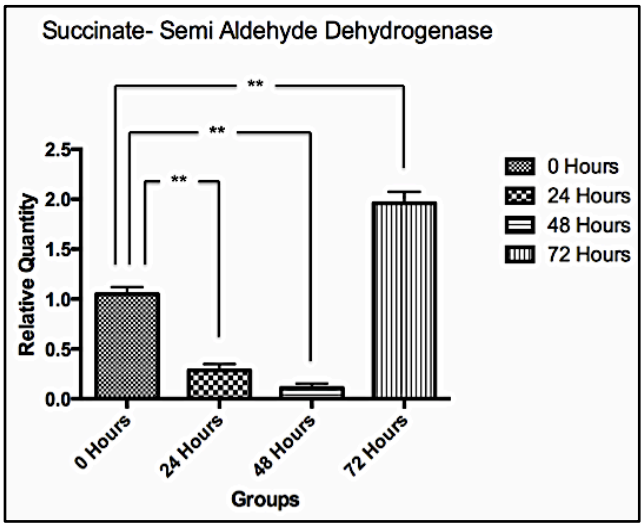

Figure 4.16: Differential Protein Expression of Succinate Semi Aldehyde Dehydrogenase. Expression detected in Control, 24 hours DTT-treated group, 48 hours DTT-treated group and 72 hours DTT-treated group. ***p*<0.01.

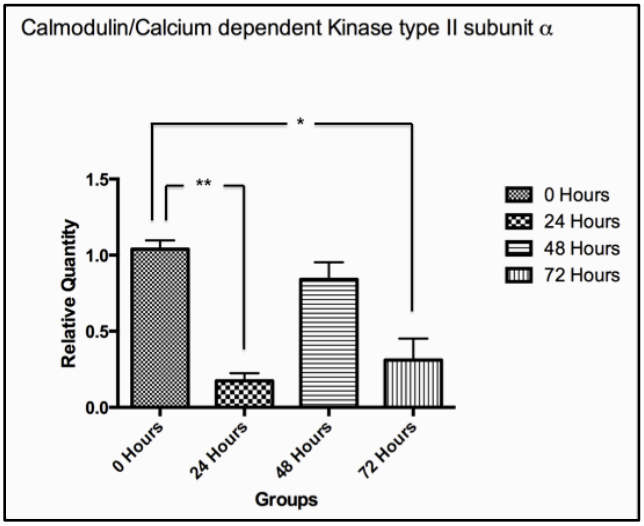

Figure 4.17: Differential Protein Expression of Calmodulin/Calcium dependent Kinase type II, subunit α. Expression detected in Control, 24 hours DTT-treated group, 48 hours DTT-treated group and 72 hours DTT-treated group. **p*<0.05, ***p*<0.01.

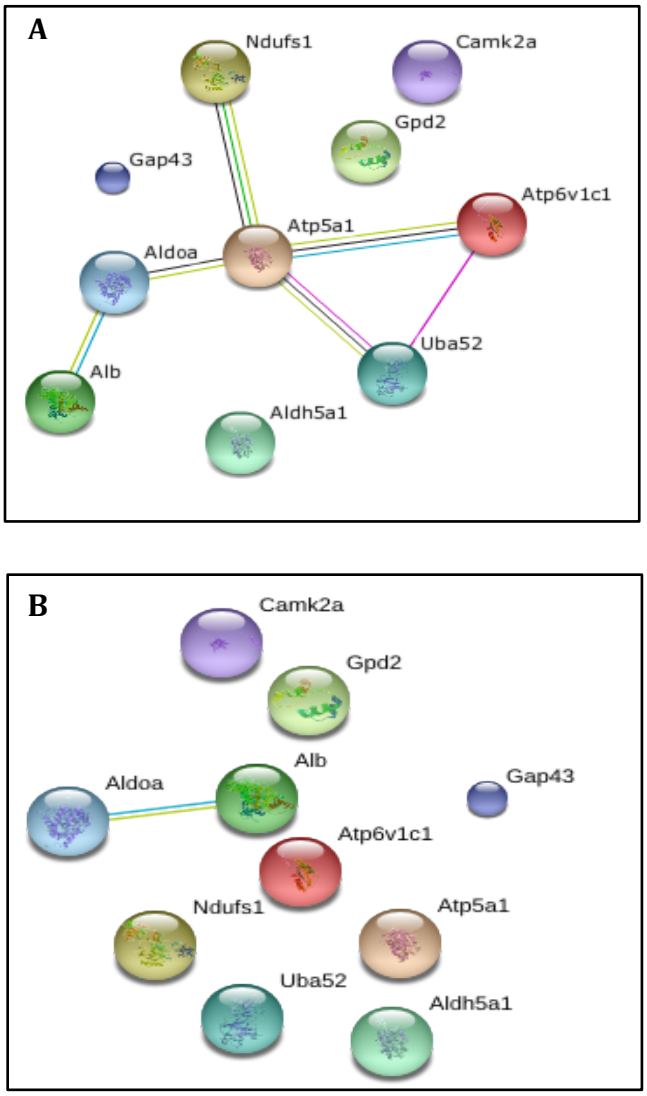

Figure 4.18: Functional association network of identified proteins in the mouse brain. A: protein-protein interaction network at medium confidence. **B:** High confidence protein-protein interaction network of identified proteins derived from the STRING database (http://string-db.org). Each protein is represented as a node with edged interactions.

4.3 Gene Expression Analysis of Amyloid Precursor Protein (APP) Isoforms and Activating Transcription Factor 6 (ATF6)

Real-Time PCR reactions were carried out to observe the relationship between ER stress sensor ATF6 and APP isoforms (Common, 695, 770) at the transcriptional level in DTT treated mRNA samples at three different time intervals (24 h, 48 h and 72 h). It was observed that the expression of APP common remained similar in the cortex, however, interestingly the expression sharply declined in the hippocampal region, with the increase in dose (Figure 4.18A and B). APP 695 levels in both the cortex and hippocampus exhibited the same pattern of expression, i.e. gradual decrease with the increase in dosage. The expression was observed to be up regulated significantly after 24 h of treatment and then gradually decreased as subsequent doses were administered (Figure 4.19A and B). APP 695 performs a neuroprotective role in the cells of the brain and is the most prominent isoform to be present in the CNS. Furthermore, in both cortex and hippocampus, mRNA levels of APP 770 after 24 h of treatment displayed a trend of significant down regulation (Figure 4.20A and B). On the other hand, ATF6 mRNA expression slightly decreased after 24 h and then was significantly up regulated after 48 h, where ER stress has reached its peak. Moreover, after 72 h, ATF6 levels were down regulated in both cortex and hippocampus (Figure 4.21A and B). ATF6 is one of the UPR branches, upon sensing ER stress, translocates into the nucleus and activates transcription of chaperone proteins for cell survival in the early stages of stress (24 h), however also induces apoptosis under sustained stress (72 h).

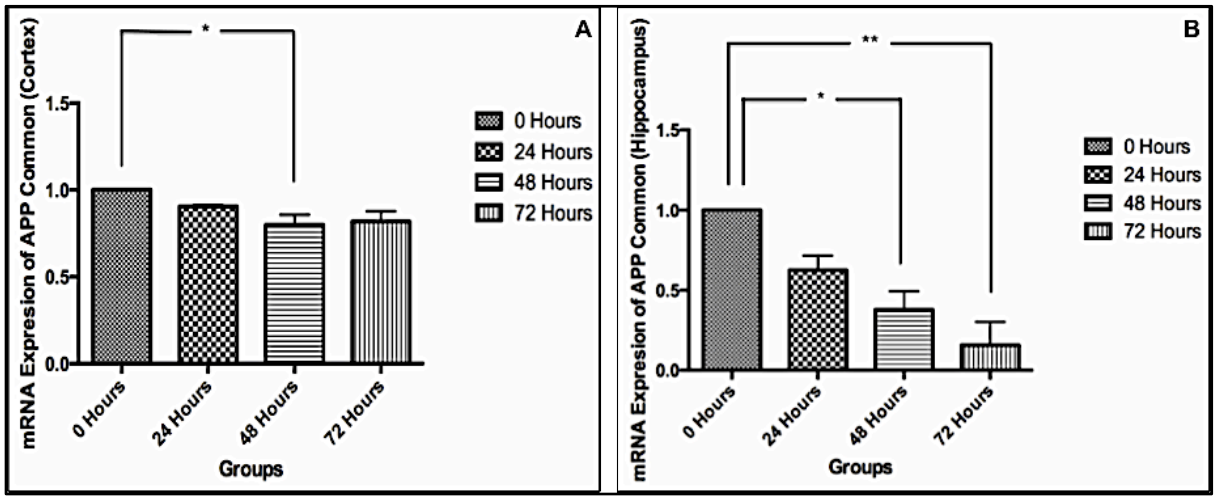

Figure 4.19: mRNA Expression of APP common in the Mouse Brain. A: Cortex **B:** Hippocampus. Lane 1: Control, Lane 2: 24 Hours DTT-Treated Group, Lane 3: 48 Hours DTT-Treated group, Lane 4: 72 Hours DTT-treated Group. **p*<0.05, ***p*<0.01.

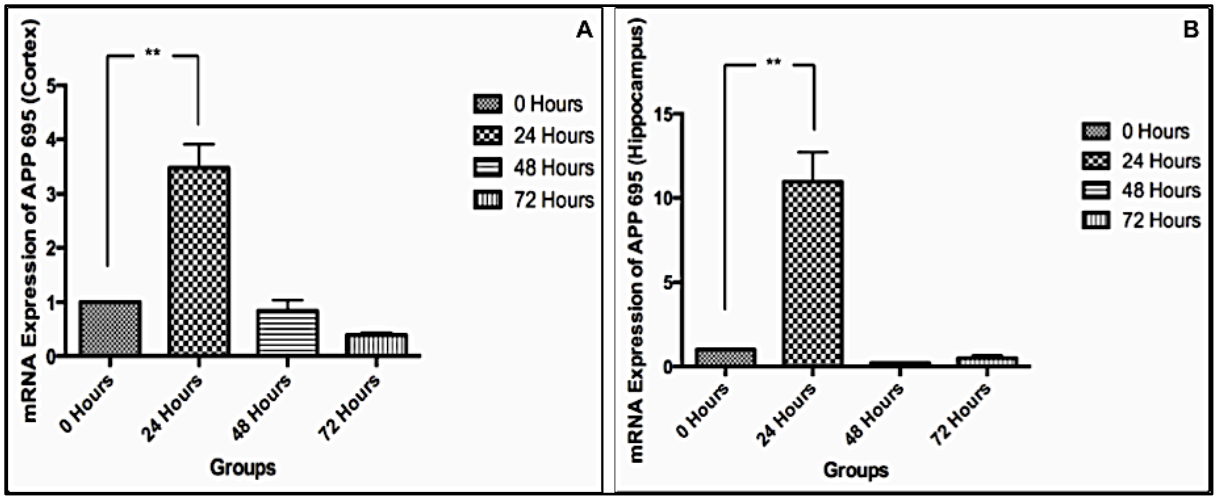

Figure 4.20: mRNA Expression of APP 695 in the Mouse Brain. A: Cortex **B:** Hippocampus. Lane 1: Control, Lane 2: 24 Hours DTT-Treated Group, Lane 3: 48 Hours DTT-Treated group, Lane 4: 72 Hours DTT-treated Group. ***p*<0.01.

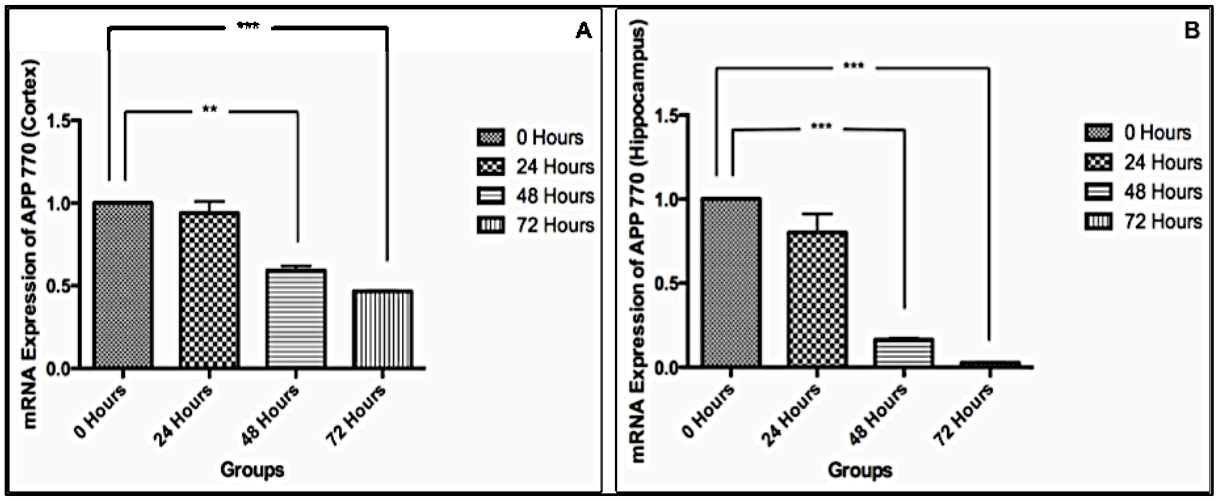

Figure 4.21: mRNA Expression of APP 770 in the Mouse Brain. A: Cortex **B:** Hippocampus. Lane 1: Control, Lane 2: 24 Hours DTT-Treated Group, Lane 3: 48 Hours DTT-Treated group, Lane 4: 72 Hours DTT-treated Group. ***p*<0.01, ****p*<0.001.

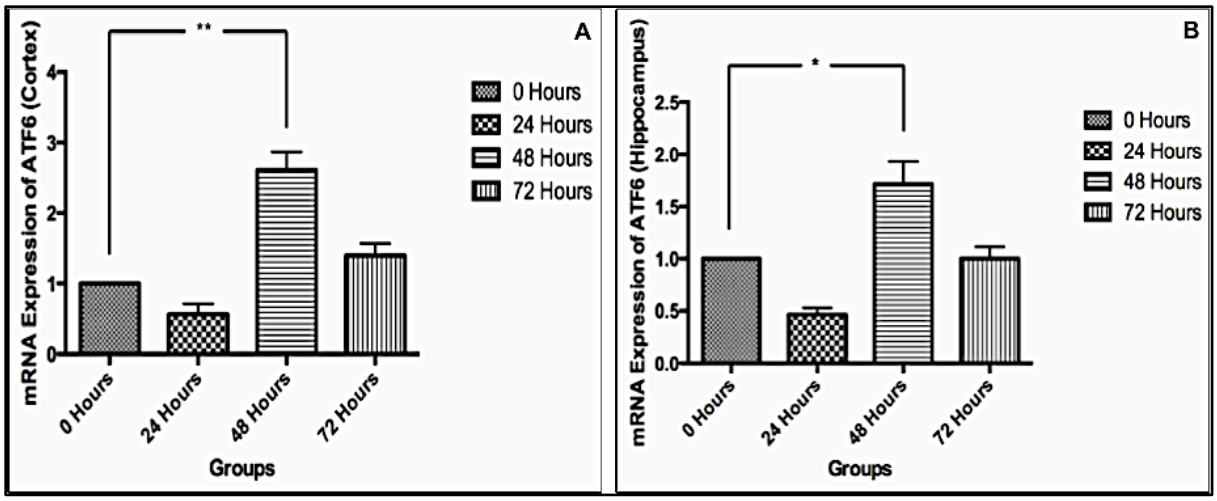

Figure 4.22: mRNA Expression of ATF6 in the Mouse Brain. A: Cortex **B:** Hippocampus. Lane 1: Control, Lane 2: 24 Hours DTT-Treated Group, Lane 3: 48 Hours DTT-Treated group, Lane 4: 72 Hours DTT-treated Group. **p*<0.05, ***p*<0.01.

Chapter 5

Discussion

The study was conducted to elucidate the complex interplay between DTT induced ER stress and subsequent amyloid beta proteotoxicity. Taking into consideration the DTT_{LD50}, doses of 50mg/kg, 75mg/kg and 100mg/kg were tested and as reflected by moderate neurodegeneration with coincident alteration in cellular architecture, the optimal dose was found to be 75mg/kg. Histological analysis carried out using cresyl violet, congo red and H&E stains confirmed the deleterious effects of DTT, showing deteriorated neuronal architecture at the later stages (72 h) of ER stress Furthermore, consistent with a previous report on ATF6 translocation into the nucleus during ER stress localization (Roussel *et al.*, 2013). Immunohistochemical analysis also revealed its nuclear localization post 48h treatment, thus indicating ER stress response initiation.

In an attempt to better understand the molecular mechanisms of chemically induced ER stress, initiation of UPR and the formulation of amyloid beta plaques, a proteomic approach was employed to examine the changes in the brain proteome profile of mice treated with DTT at three different time intervals, 24 h, 48 h and 72 h. Using quantitative intensity analysis, approximately 14 protein bands were identified following gel imaging and band detection. Significant differences in the expression of 10 proteins were observed between the 24 h treatment group and the control group, the 48 h treatment group and control group, and the 72 h treatment group and the control group, respectively. From this, 10 proteins were successfully identified via the ESI-QTOF MS/MS experiments.. The main functions of these proteins were energy metabolism and transport. The functional significances, as well as the potential roles of the differentially expressed proteins in DTT-treated mice are discussed below.

5.1 Energy Metabolism-Related Proteins

A number of proteins affected by the DTT treatment were the energy metabolism-related

proteins. Among these proteins, NADH ubiquinone oxidoreductase, ATP synthase subunit α, glycerol-3-phosphate dehydrogenase, Fructose bisphosphate aldolase A and V-type proton ATPase subunit C were up regulated in the 24 h treated groups, however were found to be down regulated in the 48 h and 72 h treatment groups. In contrast, serum albumin was observed to down regulate as the time interval of the treatment increased.

ATP is the main source of energy in vertebrate cells and can be regenerated from ADP when an increased energy supply is required. ATP synthase produces ATP from ADP in the presence of a proton gradient across the inner mitochondrial membrane, which is generated by electron transport complexes in the respiratory chain (Lee et al., 1990; Fuhrmann et al., 2013). The down-regulation of the α subunit of ATP synthase indicates a decline in ATP production. The down regulation of ATP production may be due to the protein load in the ER (Volgyi et al., 2015). Moreover, following the DTT treatment, the brain may switch to glycolysis as the primary resource for ATP production (Gilany et al., 2010), resulting in a decrease in oxidative phosphorylation. Our data showed that those proteins involved in glucose metabolism and biological oxidation were markedly influenced by DTT, which suggests that there is a decreased capacity for aerobic ATP production during ER stress in mice brain.

5.2 Neurotransmission-Related Proteins

Our study showed that the expression levels of both neuromodulin and succinate semi aldehyde dehydrogenase increased markedly at later stages of ER stress (72 h). In contrast, the expression of Calmodulin/Calcium dependent kinase type II α, had significantly increased after 48 h of treatment and declined after 72 hours. Succinate semi aldehyde dehydrogenase is a negative regulator of the inhibitory neurotransmitter, GABA (Wang et al., 2013). The GABA neurotransmitter reduces the function of hyper activated neurons. Hyperactive neurons lead to emotions like fear or anxiety, which makes succinate semi aldehyde dehydrogenase one of the key enzymes for synaptic

neurotransmission (Pearl et al., 2014). Under ER stress, if the expression declines then GABA will not be inhibited and eventually neurotransmission between neurons will come to a halt. Furthermore, if succinate semi aldehyde dehydrogenase levels have been up regulated, inhibition of GABA will be at a great extent that will lead to sustained hyperactivity of neurons (Del Pino 2015). Similarly, neuromodulin plays an important role in the nerve growth, development, repair and neurogenesis. Additionally, it also binds to calmodulin, in the absence of Ca2+ ions (Benowitz and Routtenburg, 1997). In ER stress conditions, neuromodulin incorporates in the ER and contributes to the ER protein load (Kim et al., 2006). On the other hand, calcium/calmodulin dependent kinase type-II alpha is a prominent kinase found in the central nervous system (CNS) and its function is long-term potentiation and neurotransmitter release. Moreover, ER is the reservoir of Ca2+ ions, which are released during neurotransmitter release (Liu and Murray, 2012). Under normal conditions, calmodulin binds to 4 Ca2+ ions for activation and furthermore, phosphorylates other kinases and proteases that help in autophagy. Autophagy is normally a cell survival tool, however under cellular stress, it leads to cell death (Ryan et al., 2014). Recent evidence points to the fact that ER stress triggers an efflux of Ca2+ ions into the cytoplasm, which bind to calmodulin, which becomes hyper activated that ultimately leads to sustained autophagy in the neuron that may lead to cellular apoptosis (Roe and Ren, 2013). However, the mechanisms behind neurotransmission dysfunction in ER stress remains to be further clarified.

5.3 Other ER Stress- Related Proteins

Ubiquitin- 60S ribosomal protein was also identified to be differentially expressed in our study. This enzyme plays a key role in the degradation of cellular proteins via the proteasome (Caldeira et al., 2014). Proteins that have fulfilled their cellular functions are marked with ubiquitin and are degraded by the proteasome. Degradation involves the protein to be broken down into its comprising amino acids, which are required for the production of other proteins (Jung et al., 2015). During ER stress, ubiquitin binds to the Lys residue of the misfolded proteins and activates the Endoplasmic Reticulum

associated degradation (ERAD) pathway (Castrillo and Oliver, 2016). We suggest that the down-regulation of this protein is due to the accumulation of misfolded protein aggregates, which may lead to cell apoptosis.

qRT-PCR results demonstrated a decrease in APP 770 coincident with increased ATF6 transcriptional levels post 48h treatment. It is speculated that UPR mediated transcriptional activation of pro-survival genes and suppression of functionally inconsequential genes underlies the down regulation of APP 770 (Roussel et al., 2013). It is conceivable that ATF6 mediated down regulation of APP 770 is responsible for ATF6 associated anti apoptotic response, since amyloid beta proteotoxicity is known to govern AD associated neurodegeneration. In the present study, the expression of neuroprotective APP 695 has been observed to steadily decline in all stages of ER stress, which coincides with pattern appeared in related work (Rohan *et al*., 1997; Kang *et al*., 1990).

5.4 Conclusion

There is strong evidence for activation of ER-stress-responsive pathways in a range of neurological disorders. What remains to be discovered is how successful will the strategies be that target these responses, in the treatment of neurological disorders. This study has revealed an insight on the basic molecular mechanism underlying the relationship between UPR and neurodegeneration. From this preliminary data, we can conclude that environmental toxicity may lead to a build up of misfolded proteins in the ER, which causes a temporary halt in all cellular processes. Moreover, continuous stress leads the ER stress sensors to activate apoptotic pathways. Interestingly, it is noted that during the early stages of stress (24 h), the sensor levels are high and during the late stages its completely minimal (72 h). Research into unfolded-protein-response signaling has matured to a point at which small-molecule inhibitors of its components are under development, which can be used as bio-markers for early onset neurological disorders like AD, PD or ALS.

Chapter 6

References

- Asfari, M., Janjic, D., Meda, P., Li, G., Halban, P. A., & Wollheim, CB. Establishment of 2-mercaptoethanol-dependent differentiated insulin-secreting cell lines. Endocrinology. 1992. 130:167–178.
- Nijholt, D., De Kimpe, L., L Elfrink, H., JM Hoozemans, J., & Scheper, W. (2011). Removing protein aggregates: the role of proteolysis in neurodegeneration. Current Medicinal Chemistry, 18(16), 2459-2476.
- Benowitz, L. I., Routtenberg, A. (1997). GAP-43: an intrinsic determinant of neuronal development and plasticity. Trends in neurosciences, 20(2), 84-91.
- Bernales, S., Papa, F. R., & Walter, P. (2006). Intracellular signaling by the unfolded protein response. Annual Review of Cell and Developmental Biology. 22, 487-508.
- Bertolotti, A., Ron, D. (2001). Alterations in an IRE1-RNA complex in the mammalian unfolded protein response. Journal of Cell Science, 114(17), 3207-3212.
- Butterfield, D. A. (1997). β-Amyloid-associated free radical oxidative stress and neurotoxicity: implications for Alzheimer's disease. Chemical Research In Toxicology, 10(5), 495-506.
- Butterfield, D. A., Boyd‐Kimball, D. (2004). Amyloid β‐Peptide (1‐42) Contributes to the Oxidative Stress and Neurodegeneration Found in Alzheimer Disease Brain. Brain Pathology, 14(4), 426-432.
- Caldeira, M. V., Salazar, I. L., Curcio, M., Canzoniero, L. M., & Duarte, C. B. (2014). Role of the ubiquitin–proteasome system in brain ischemia: Friend or foe? Progress In Neurobiology, 112, 50-69.

- Calfon, M., Zeng, H., Urano, F., Till, J. H., Hubbard, S. R., Harding, H. P., & Ron, D. (2002). IRE1 couples endoplasmic reticulum load to secretory capacity by processing the XBP-1 mRNA. Nature, 415(6867), 92-96.
- Campbell, A., Smith, M. A., Sayre, L. M., Bondy, S. C., & Perry, G. (2001). Mechanisms by which metals promote events connected to neurodegenerative diseases. Brain Research Bulletin, 55(2), 125-132.
- Castellani, R. J., Moreira, P. I., Perry, G., & Zhu, X. (2012). The role of iron as a mediator of oxidative stress in Alzheimer disease. Biofactors, 38(2), 133-138.
- Castrillo, J. I., Oliver, S. G. (2015). Alzheimer's as a Systems-Level Disease Involving the Interplay of Multiple Cellular Networks. Systems Biology of Alzheimer's Disease, 3-48.
- Chen, R., Dai, R. Y., Duan, C. Y., Liu, Y. P., Chen, S. K., Yan, D. M., Chen, C. N., Wei, M., & Li, H. (2011). Unfolded protein response suppresses cisplatin-induced apoptosis via autophagy regulation in human hepatocellular carcinoma cells. Folia Biologica. 57(3), 87-95.
- Cleland, W. W. (1964). Dithiothreitol, a new protective reagent for SH groups. Biochemistry, 3(4), 480-482.
- Credle, J.J., Finer-Moore, J.S., Papa, F.R., Stroud, R.M., & Walter, P. (2005). On the mechanism of sensing unfolded protein in the endoplasmic reticulum. Proceedings of the National Academy of Sciences.102, 18773–18784.
- Crichton, R. R., Dexter, D. T., & Ward, R. J. (2012). Brain iron metabolism and its perturbation in neurological diseases. Journal of Neurotransmission. 118(3):301-14.
- Del Pino, J., Frejo, M. T., Baselga, M. J. A., Moyano, P., & Díaz, M. J. (2015). Impaired glutamatergic and GABAergic transmission by amitraz in primary hippocampal cells. Neurotoxicology And Teratology, 50, 82-87.

- Deng, Y., Srivastava, R., & Howell, S. H. (2013). Endoplasmic reticulum (ER) stress response and its physiological roles in plants. International Journal Of Molecular Sciences, 14(4), 8188-8212.
- Dixon, S. J., & Stockwell, B. R. (2014). The role of iron and reactive oxygen species in cell death. Nature Chemical Biology, 10(1), 9-17.
- Drake, J., Link, C. D., &Butterfield, D. A. (2003). Oxidative stress precedes fibrillar deposition of Alzheimer's disease amyloid β-peptide (1–42) in a transgenic *Caenorhabditis elegans* model. Neurobiology Of Aging, 24(3), 415-420.
- Dyrks, T., Dyrks, E., Hartmann, T., Masters, C., & Beyreuther, K. (1992). Amyloidogenicity of _A4 and _A4-bearing amyloid protein precursor fragments by metal-catalyzed oxidation. Journal of Biological Chemistry. 267:18210–18217
- Engidawork, E., Gulesserian, T., Seidl, R., Cairns, N., & Lubec, G. (2001). Expression of apoptosis related proteins in brains of patients with Alzheimer's disease. Neuroscience Letters, 303(2), 79-82.
- Fuhrmann, D. C., Wittig, I., Heide, H., Dehne, N., & Brüne, B. (2013). Chronic hypoxia alters mitochondrial composition in human macrophages. Biochimica et Biophysica Acta (BBA)-Proteins and Proteomics, 1834(12), 2750-2760.
- Gao, W., Fu, Y., Yu, C., Wang, S., Zhang, Y., Zong, C., & Wang, X. (2014). Elevation of NR4A3 Expression and Its Possible Role in Modulating Insulin Expression in the Pancreatic Beta Cell. PloS one, 9(3), e91462.
- Greenough, M. A., Camakaris, J., & Bush, A. I. (2013). Metal dyshomeostasis and oxidative stress in Alzheimer's disease. Neurochemistry International, 62(5), 540-555.
- Hattori, M., Tsukahara, F., Furuhata, Y., Tanahashi, H., Hirose, M., Saito, M., & Sakaki, Y. (1997). A novel method for making nested deletions and its application for sequencing of a 300 kb region of human APP locus. Nucleic Acids Research, 25(9), 1802-1808.

- Haze, K., Yoshida, H., Yanagi, H., Yura, T., & Mori, K. (1999). Mammalian transcription factor ATF6 is synthesized as a transmembrane protein and activated by proteolysis in response to endoplasmic reticulum stress. Molecular Biology Of The Cell, 10(11), 3787-3799.
- Hohmeier, H. E., Mulder, H., Chen, G., Henkel-Rieger, R., Prentki, M., & Newgard, C. B. (2000). Isolation of INS-1-derived cell lines with robust ATP-sensitive K+ channel-dependent and -independent glucose-stimulated insulin secretion. Diabetes. 49(3):424–30.
- Hoozemans, J. J. M., Veerhuis, R., Van Haastert, E. S., Rozemuller, J. M., Baas, F., Eikelenboom, P., & Scheper, W. (2005). The unfolded protein response is activated in Alzheimer's disease. Acta Neuropathologica, 110(2), 165-172.
- Hoozemans, J. J., van Haastert, E. S., Nijholt, D. A., Rozemuller, A. J., Eikelenboom, P., & Scheper, W. (2009). The unfolded protein response is activated in pretangle neurons in Alzheimer's disease hippocampus. The American Journal Of Pathology, 174(4), 1241-1251.
- Høyer-Hansen, M., Jäättelä, M. (2007). Connecting endoplasmic reticulum stress to autophagy by unfolded protein response and calcium. Cell Death & Differentiation, 14(9), 1576-1582.
- Jung, E. S., Hong, H., Kim, C., & Mook-Jung, I. (2015). Acute ER stress regulates amyloid precursor protein processing through ubiquitin-dependent degradation. Scientific Reports, 5;5:8805.
- Kang, J., Müller-Hill, B. (1990). Differential splicing of Alzheimer's disease amyloid A4 precursor RNA in rat tissues: PreA4 695 mRNA is predominantly produced in rat and human brain. Biochemical And Biophysical Research Communications, 166(3), 1192-1200.
- Kim, S. J., Zhang, Z., Hitomi, E., Lee, Y. C., & Mukherjee, A. B. (2006). Endoplasmic reticulum stress-induced caspase-4 activation mediates apoptosis and neurodegeneration in INCL. Human Molecular Genetics, 15(11), 1826-1834.

- Kitaguchi, N., Takahashi, Y., Tokushima, Y., Shiojiri, S., & Ito, H. (1988). Novel precursor of Alzheimer's disease amyloid protein shows protease inhibitory activity. Nature, 331(6156), 530-532.
- Kitaguchi, N., Tokushima, Y., Oishi, K., Takahashi, Y., Shiojiri, S., Nakamura, & Ito, H. (1990). Determination of amyloid β protein precursors harboring active form of proteinase inhibitor domains in cerebrospinal fluid of Alzheimer's disease patients by trypsin-antibody sandwich ELISA. Biochemical And Biophysical Research Communications, 166(3), 1453-1459.
- Kitamura, K., Taki, M., Tanaka, N., & Yamashita, I. (2011). Fission yeast Ubr1 ubiquitin ligase influences the oxidative stress response via degradation of active Pap1 bZIP transcription factor in the nucleus. Molecular Microbiology, 80(3), 739-755.
- Kitamura, Y., Shimohama, S., Kamoshima, W., Ota, T., Matsuoka, Y., Nomura, Y., & Taniguchi, T. (1998). Alteration of proteins regulating apoptosis, Bcl-2, Bcl-x, Bax, Bak, Bad, ICH-1 and CPP32, in Alzheimer's disease. *Brain research, 780*(2), 260-269.
- Klunk, W. E., Xu, C. J., McClure, R. J., Panchalingam, K., Stanley, J. A., & Pettegrew, J. W. (1997). Aggregation of -amyloid peptide is promoted by membrane phospholipid metabolites elevated in Alzheimer's disease brain. Journal of Neurochemistry. 69: 266–272.
- Kozutsumi, Y., Segal, M., Normington, K., Gething, M. J., & Sambrook, J. (1988). The presence of malfolded proteins in the endoplasmic reticulum signals the induction of glucose-regulated proteins. Nature. 332(6163):462-4.
- Lambert, M., Barlow, A., Chromy, B., Edwards, C., Freed, R., Liosatos, M., & Viola, K. (1998). Diffusible, nonfibrillar ligands derived from Aβ1–42 are potent central nervous system neurotoxins. Proceedings Of The National Academy Of Sciences, 95(11), 6448-6453.

- LeBlanc, A., Chen, H., Autilio-Gambetti, L., & Gambetti, P. (1991). Differential APP gene expression in rat cerebral cortex, meninges, and primary astroglial, microglial and neuronal cultures. FEBS letters, 292(1), 171-178.
- Li, J., Chen, Z., Gao, L. Y., Colorni, A., Ucko, M., Fang, S., & Du, S. J. (2015). A transgenic zebrafish model for monitoring xbp1 splicing and endoplasmic reticulum stress in vivo. Mechanisms Of Development. 137:33-44.
- Liu, X. B., Murray, K. D. (2012). Neuronal excitability and calcium/calmodulin-dependent protein kinase type II: Location, location, location. Epilepsia, 53(1), 45-52.
- Maly, D. J., Papa, F. R. (2014). Druggable sensors of the unfolded protein response. Nature Chemical Biology, 10(11), 892-901.
- Mantyh, P. W., Ghilardi, J. R., Rogers, S., DeMaster, E., Allen, C. J., Stimson, E. R., & Maggio, J. E. (1993). Aluminum, Iron, and Zinc Ions Promote Aggregation of Physiological Concentrations of β-Amyloid Peptide. Journal Of Neurochemistry, 61(3), 1171-1174.
- Miyazaki, J., Araki, K., Yamato, E., Ikegami, H., Asano, T., Shibasaki, Y., Oka, Y., & Yamamura, K. (1990). Establishment of a pancreatic beta cell line that retains glucose-inducible insulin secretion: special reference to expression of glucose transporter isoforms. Endocrinology.127:126–132.
- Moore, K.A.; Hollien, J. (2012) The unfolded protein response in secretory cell function. Annual Review of Genetics. 46, 165–183.
- Nishimoto, I., Okamoto, T., Matsuura, Y., Takahashi, S., Okamoto, T., Murayama, Y., & Ogata, E. (1993). Alzheimer amyloid protein precursor complexes with brain GTP-binding protein Go. Nature 362: 75-79.
- Pearl, P. L., Schreiber, J., Theodore, W. H., McCarter, R., Barrios, E. S., Yu, J., & Gibson, K. M. (2014). Taurine trial in succinic semialdehyde dehydrogenase deficiency and elevated CNS GABA. Neurology, 82(11), 940-944.

- Preece, P., Virley, D. J., Costandi, M., Coombes, R., Moss, S. J., Mudge, A. W., & Cairns, N. J. (2004). Amyloid precursor protein mRNA levels in Alzheimer's disease brain. Molecular Brain Research, 122(1), 1-9.
- Priller, C., Bauer, T., Mitteregger, G., Krebs, B., Kretzschmar, H. A., & Herms, J. (2006). Synapse formation and function is modulated by the amyloid precursor protein. The Journal of Neuroscience, 26(27), 7212-7221.
- Roe, N. D., Ren, J. (2013). Oxidative activation of Ca2+/calmodulin-activated kinase II mediates ER stress-induced cardiac dysfunction and apoptosis. American Journal of Physiology-Heart and Circulatory Physiology, 304(6), 828-839.
- Ron, D., Walter, P. (2007). Signal integration in the endoplasmic reticulum unfolded protein response. Nature Reviews Molecular Cell Biology, 8(7), 519-529.
- Rouault, T. A. (2013). Iron metabolism in the CNS: implications for neurodegenerative diseases. Nature Reviews Neuroscience, 14(8), 551-564.
- Roussel, B. D., Kruppa, A. J., Miranda, E., Crowther, D. C., Lomas, D. A., & Marciniak, S. J. (2013). Endoplasmic reticulum dysfunction in neurological disease. The Lancet Neurology, 12(1), 105-118.
- Ruggiano, A., Foresti, O., & Carvalho, P. (2014). ER-associated degradation: Protein quality control and beyond. The Journal Of Cell Biology, 204(6), 869-879.
- Ryan, A. J., Larson-Casey, J. L., He, C., Murthy, S., & Carter, A. B. (2014). Asbestos-induced Disruption of Calcium Homeostasis Induces Endoplasmic Reticulum Stress in Macrophages. Journal Of Biological Chemistry, 289(48), 33391-33403.
- Ryoo, H. D., Domingos, P. M., Kang, M. J., & Steller, H. (2007). Unfolded protein response in a Drosophila model for retinal degeneration. The EMBO Journal, 26(1), 242-252.

- Scheper, W., Hoozemans, J. J. (2015). The unfolded protein response in neurodegenerative diseases: a neuropathological perspective. Acta Neuropathologica, 130(3):315-31.
- Schindler, A. J., Schekman, R. (2009). In vitro reconstitution of ER-stress induced ATF6 transport in COPII vesicles. Proceedings of the National Academy of Sciences. 106:17775–17780.
- Schuiki, I., Zhang, L., & Volchuk, A. (2012). Endoplasmic Reticulum Redox State Is Not Perturbed by Pharmacological or Pathological Endoplasmic Reticulum Stress in Live Pancreatic β-Cells. PloS one, 7(11), e48626.
- Shen, J., Chen, X., Hendershot, L., & Prywes, R. (2002). ER stress regulation of ATF6 localization by dissociation of BiP/GRP78 binding and unmasking of Golgi localization signals. Developmental Cell, 3(1), 99-111.
- Subjeck, J. R., Shyy, T. T. (1986). Stress protein systems of mammalian cells. American Journal of Physiology-Cell Physiology, 250(1), 1-17.
- Taylor, R. C., Berendzen, K. M., & Dillin, A. (2014). Systemic stress signaling: understanding the cell non-autonomous control of proteostasis. Nature Reviews Molecular Cell Biology 15(3):211-17.
- Varadarajan, S., Yatin, S., Aksenova, M., & Butterfield, D. A. (2000). Alzheimer's amyloid _-peptide-associated free radical oxidative stress and neurotoxicity. Journal of Structural Biology. 30:184–208.
- Volgyi, K., Juhász, G., Kovacs, Z., & Penke, B. (2015). Dysfunction of Endoplasmic Reticulum (ER) and Mitochondria (MT) in Alzheimer's Disease: The Role of the ER-MT Cross-Talk. Current Alzheimer Research, 12(7), 655-672.
- Wang, S., Kaufman, R. J. (2012). The impact of the unfolded protein response on human disease. The Journal Of Cell Biology, 197(7), 857-867.
- Wang, X. L., Liang, J. Y., Liu, R. Z., Dong, Z., & Yu, S. Y. (2013). The expression of succinate semialdehyde dehydrogenase in the caudal part of the spinal trigeminal nucleus is down-regulated after electrical stimulation of the dura

mater surrounding the superior sagittal sinus in conscious rats. Neuroscience, 248:145-153.

- Wolfe, M. S., De Los Angeles, J., Miller, D. D., Xia, W., Selkoe, D. J. (1999). Are presenilins intramembrane-cleaving proteases? Implications for the molecular mechanism of Alzheimer's disease. Biochemistry, 38(35), 11223-11230.
- Ye, J., Rawson, R. B., Komuro, R., Chen, X., Dave, U. P., Prywes, R., Brown, M. S., Goldstein, J. L. (2000). ER stress induces cleavage of membrane-bound ATF6 by the same proteases that process SREBPs. Molecular Cell. 6, 1355–1364.
- Yoshida, H., Matsui, T., Yamamoto, A., Okada, T., & Mori, K. (2001). XBP1 mRNA is induced by ATF6 and spliced by IRE1 in response to ER stress to produce a highly active transcription factor. Cell, 107(7), 881-891.
- Youdim, M. (1988). Iron in the brain: implications for Parkinson's and Alzheimer's diseases. The Mount Sinai Journal Of Medicine, New York, 55(1), 97-101.
- Zheng, H., and Koo, E. H. (2006). The amyloid precursor protein: beyond amyloid. Molecular Neurodegeneration, 1(1), 5.

Appendix

Poster Presentation

Zahra Mahmood, Sara Ahmed, Touqeer Ahmed, Saadia Zahid. (2015). Effects of Chemical Toxicants on Mouse Brain. International Conference on Recent Innovations in Pharmaceutical Sciences (*ICRIPS*).

Abstract

Oxidative stress has been implicated as a triggering factor of many neurodegenerative disorders, including Alzheimer's disease (AD). Aluminum (Al) is the third most abundant element in the Earth's crust and is an established neurotoxicant that leads to the production of reactive oxygen species (ROS). Dithiothreitol (DTT) is a strong reducing agent and when it undergoes oxidation it converts into a very stable superoxide and causes the production of ROS. Furthermore, it disintegrates the disulphide bridges in proteins, causing them to lose their conformation and becoming denatured. Thus, DTT has also been implicated as an Unfolded Protein Response (UPR) initiator in the endoplasmic reticulum. This study has been conducted to determine whether DTT can cause neurodegeneration as well as initiating the Unfolded Protein Response (UPR). In house mice models of neurotoxicity were prepared by administering $AlCl_3$ (600 mg/kg for 15 days) and DTT (50, 75 and 100 mg/kg for 3 days). After the duration of treatment, the mice underwent perfusion and were sacrificed respectively. The brains were collected and histology was performed. Histology involved the usage of Congo Red and Cresyl Violet stains. The control samples were compared with the samples of $AlCl_3$ and DTT. Neurodegeneration was visible in both $AlCl_3$ and DTT samples. However, the extent of neurodegeneration in the DTT samples (75 and 100 mg/kg) is much more than in the $AlCl_3$ samples. The present study indicates that DTT has the potential of causing a higher extent of neurodegeneration in a much shorter duration of time.